REPORT DOCUMENTATION PAGE

Form Approved OMB No. 0704-0188

1. REPORT DATE *(DD-MM-YYYY)*	2. REPORT TYPE	3. DATES COVERED *(From – To)*
24-11-2008	Final Report	1 November 2005 - 09 June 2010

4. TITLE AND SUBTITLE

Femtosecond Lasers with Diode Pumping for Using in Precision Metrology and Optical Fiber Communication

5a. CONTRACT NUMBER
FA8655-03-D-0001, Delivery Order 0028

5b. GRANT NUMBER
CDRF 05-9001

5c. PROGRAM ELEMENT NUMBER
61102F

6. AUTHOR(S)

Dr. Vladimir I Denisov

5d. PROJECT NUMBER

5d. TASK NUMBER

5e. WORK UNIT NUMBER

7. PERFORMING ORGANIZATION NAME(S) AND ADDRESS(ES)

Institute of Laser Physics
Ac. Lavrentyeva Ave.
Novosibirsk 630090
Russia

8. PERFORMING ORGANIZATION REPORT NUMBER

PROJECT # RUP2-1510-NO-05

9. SPONSORING/MONITORING AGENCY NAME(S) AND ADDRESS(ES)

EOARD
Unit 4515 BOX 14
APO AE 09421

10. SPONSOR/MONITOR'S ACRONYM(S)

11. SPONSOR/MONITOR'S REPORT NUMBER(S)

EOARD Task 05-9001

12. DISTRIBUTION/AVAILABILITY STATEMENT

Approved for public release; distribution is unlimited.

13. SUPPLEMENTARY NOTES

14. ABSTRACT:

The recent merge of precision optical frequency metrology and ultrafast laser technology has made a profound impact to a number of scientific disciplines, including fundamental physical tests, precision spectroscopy in chemistry, biology, and material science, metrological support in space science, and coherent quantum control. For the area of frequency metrology on which this proposal is focused, we expect a significant increase in the stability and accuracy of frequency standards is needed and is ready to be developed, especially in light with the identification of optically based transitions with extremely high quality factors. Phase coherent connection between the optical and microwave spectral regions has now been established with direct optical frequency synthesis, with a qualitatively new regime being developed owing to the introduction of precise femtosecond laser based optical frequency comb technology. At the present time, optical fiber communication lines (OFCL) are widely used. One way for increasing the OFCL transmission capacity is the spectral separation of channels. For this, a stable chain of working optical frequencies is necessary. It is convenient to use the radiation from a stabilized femtosecond laser as such a frequency chain. The prospects for using such femtosecond synthesizers for OFCL are confirmed by the fact that there are many publications on this theme. .In first stage we propose to develop an ideal alternative system based on femtosecond diode-pumped ytterbium-laser. The use of diode pumping for crystalline lasers makes it possible to construct compact, highly efficient, as well as economical laser systems. The relatively low thermal load and compactness of the laser system help to create stable optical resonators and to obtain highly reliable laser operating parameters. A femtosecond comb system based on a Yb-laser will be much more compact and economical than its Ti:S counterpart. We plan to investigate spectral broadening of the Yb femtosecond laser for creating of Yb femtosecond comb. In continuation of this project the researches of the Cr:Forsterite laser are assumed.

15. SUBJECT TERMS

EOARD, Femtosecond pulses, Laser physics, ultrashort pulse interactions

16. SECURITY CLASSIFICATION OF:			17. LIMITATION OF ABSTRACT	18, NUMBER OF PAGES	19a. NAME OF RESPONSIBLE PERSON
a. REPORT	b. ABSTRACT	c. THIS PAGE			A. GAVRIELIDES
UNCLAS	UNCLAS	UNCLAS	SAR	39	19b. TELEPHONE NUMBER *(Include area code)* +44 (0)1895 616205

U.S. Civilian Research and Development Foundation
1530 Wilson Boulevard, Arlington, VA 22209

GRANT ASSISTANCE PROGRAM

FINAL TECHNICAL REPORT

Femtosecond Lasers with Diode Pumping for Using in Precision Metrology and Optical Fiber Communication

(PROJECT # RUP2-1510-NO-05)
CDRF 05-9001

Project Director:	**Dr. Vladimir Denisov**
Principal Organization:	**Institute of Laser Physics, SB RAS**
Address:	**13/3 Ac. Lavrentyeva Ave.** **Novosibirsk 630090** **Russian Federation**
Phone:	**+7(383)3333478**
Fax:	**+7(383) 3332067**
Email:	**denisov@laser.nsc.ru**

Contents

1. Summary

The work on stabilization of the parameters of the femtosecond Cr:Forsterite laser has been accomplished. For complete stabilization of the femtosecond comb one needs to control its absolute frequency. To realize this we use either angle-tilted mirror or pump intensity modulator. As a result a mechanically stable femtosecond forsterite laser with average output power of ~500 mW, pulse duration of ~40 fs and pulse repetition rate of 100 MHz has been developed. Work on increasing the Cr:Forsterite laser repetition rate from 100 MHz up to 200 – 300 MHz has been carried out.

We report on initial results of the development of a diode-laser-pumped Yb femtosecond laser for applications in femtosecond optical clock and optical frequency synthesizers. Various configurations of the laser cavity have been developed and analyzed.

Investigations of ability to achieve of femtosecond operating regime in Yb:KYW based laser with 300-500 MHz repetition rate using a multimode fiber-coupled laser as a pump source was carried out. Laser diode system UM3000/M10/CB TEC (Unique-mode) was used as pump source. Semiconductor saturable mirror (SESAM) and mirrors with negative dispersion (GTI) were utilized. Unstable operating regime was achieved.

Theoretical investigation of pulse train spectral envelope in highly nonlinear fibers was performed by modified nonlinear Srodinger equation (NLSE), describing single pulse propagation. Numerical solutions according to experimental parameters were found by use of self-split Fourier method (SSFM).

Numerical investigations of the femtosecond mode-locked laser radiation spectrum broadened in an optical fiber with the effect of incoming radiation noise are presented. It was found that the pulse train intensity and shape stability, i.e fluctuations of incoming radiation, strongly affect the output spectral characteristics; such as the spectral envelope and amplitudes of equidistant components in a femtosecond comb.

2. Introduction

The field of precision optical frequency measurements has undergone a major revolution during recent years due to the development of highly accurate frequency combs based on ultrashort pulse mode-locked lasers. Most of this work has taken advantage of the highly–developed Ti:Sapphire laser which either directly or in combination with nonlinear frequency broadening schemes can provide octave spanning continua. Locking both the offset frequency and repetition frequency of the resulting frequency comb to an atomic clock has permitted the development of absolute optical frequency references in the visible to near infrared wavelength regions. The application of ultrashort pulse lasers operating at wavelengths longer than that of the Ti:Sapphire laser appears promising, for example, to establish time and frequency standards in the infrared for telecommunications by use of highly stable optical combs. Development of systems for frequency interval measurements based on a frequency comb is also of particular interest for frequency synthesis and metrology in the infrared. In such systems an octave spanning continuum is not mandatory and generally only a stabilization of the pulse repetition rate is required which is routinely attainable in most cases. If necessary, stabilization of the absolute frequency is achieved by locking to an optical reference.

In comparison to diode and fiber laser a solid state laser on the forsterite crystal (Cr^{4+}:Mg_2SiO_4 or Cr:F) have a number of advantages. A broad gain linewidth of the active medium allows generation of pulses shorter than 15 fs and energetic characteristics of Cr:F make possible to obtain hundreds of milliwatts of average output power. Besides, the laser generates in the vicinity to the zero dispersion region of silica fibers which means that the laser pulses can be transferred over large distances without distortions via optical fiber lines. A spectrum of equidistant frequencies in the range of 1 – 2 μm can be obtained by means of the laser spectrum broadening in special optical fibers. This spectral range is of strong demand both for metrology (as in this band there are frequency lines of widely used optical frequency standards, e.g. iodine stabilized Nd:YAG laser at 1.06 μm and acetylene stabilized diode laser at 1.5 μm) and optical fiber communication lines. A possibility to use fiber lasers for pumping and chirped mirrors for the crystal dispersion compensation permits to build a compact and reliable source of femtosecond pulses.

One of the main problems with femtosecond solid-state ytterbium lasers is the pump source. Powerful sources (> 4 W) with diffraction limited output are not available on the market. Multimode-fiber-coupled laser diodes have low power stability as well as poor beam quality and cannot be focused into a spot small enough for effective Kerr-lens mode-locking. To the best of our knowledge there is no published works on KLM ytterbium femtosecond lasers with multimode pumping. Stable femtosecond generation without saturable semiconductor mirror

(SESAM) has been reported only in two published papers where the pump source has been either single-emitter laser diode or single-mode-fiber-coupled laser diode. It is known from publications that femtosecond regime in Yb-based lasers is quite critical to angular distribution and quality of focusing of pump beam, resonator adjustment and so on in comparison with lasers based on the Ti:S crystal. Therefore semiconductor saturable mirror (SESAM) and pump source with diffractive divergence (at least in one plane) usually used to reach stable femtosecond operation. According to the specifications, the pump source UM3000/M10/CB TEC by Unique-mode company is considered to partially meet the requirements for building the femtosecond laser with high repetition rate. The suitability of the pump laser has to be verified experimentally, i.e. it is necessary to measure the Yb:KYW laser threshold, slope efficiency in the different cavity configurations, to test the power supply unit and the thermo-controller.

Considering a promising perspectives of this technique for high-precision spectroscopy and metrology, it seems important to investigate both spectral envelope and noise characteristics of broadened spectrum.

Numerical solution of pulse propagating in HNLF DDF differs from the typical cases when fiber is uniform. Since fiber parameters differ along the fiber it is necessary to modify nonlinear Shrödinger equation according to the numerical method used in calculation.

While noise characteristics of a stationary pulse trains, generated by a stable mode-locked lasers, are studied thoroughly, there are still a lot of questions in regard to the influence of nonlinear and dispersion effects in optical fibers. We present a numerical model and theoretical results related to the spectral distortions of a pulse train with amplitude fluctuations, propagating through a fiber.

3. Technical Description

3-a. Creation of a femtosecond optical frequency synthesizers based on the femtosecond Cr:Forsterite

A conventional Z-fold configuration of Cr:F laser has been used with two 10 cm radii-of-curvature concave mirrors placed at a folding angle of 32° to compensate astigmatism of the Brewster-cut Cr:F crystal. The gain crystal was 17 mm long and introduced positive group-delay dispersion of 680 fs² per round trip. A pair of SF6 prisms was used to control dispersion in the cavity. The optimal prism separation for the stable mode-locking was found experimentally to be 30 cm. The Cr:F crystal was mounted in a brass holder whose temperature was maintained at 10°C to decrease the lasing threshold and was pumped by a commercial 10 W 1.06 mkm Yb-fiber laser with the typical amplitude noise level of 1% rms.

The work on stabilization of the parameters of the femtosecond Cr:Forsterite laser has been accomplished. First, all mechanically unstable and sensitive to alignment opto-mechanical elements were found and replaced by more rigid and precise ones. Then all the cavity elements were mounted on a steel breadboard with high acoustics isolation. To prevent the air flow the laser cavity was covered with a box and the forsterite crystal was purged with dry nitrogen to avoid water condensation at temperatures below 15°C. The laser crystal temperature was kept at necessary point by a thermo-electric cooler with accuracy of 0.1°C. For the pulse repetition rate adjustment one cavity mirror was glued on a piezo-actuator which, in turn, was firmly fixed on a stable non-aligned mount. The first frequency resonance of such system was measured at ~30 kHz. For complete stabilization of the femtosecond comb one needs to control its absolute frequency. To realize this we use either angle-tilted mirror or pump intensity modulator.

As a result a mechanically stable femtosecond forsterite laser with average output power of ~500 mW, pulse duration of ~40 fs and pulse repetition rate of 100 MHz has been developed (Fig.1). Work on increasing the Cr:Forsterite laser repetition rate from 100 MHz up to 200 – 300 MHz has been carried out.

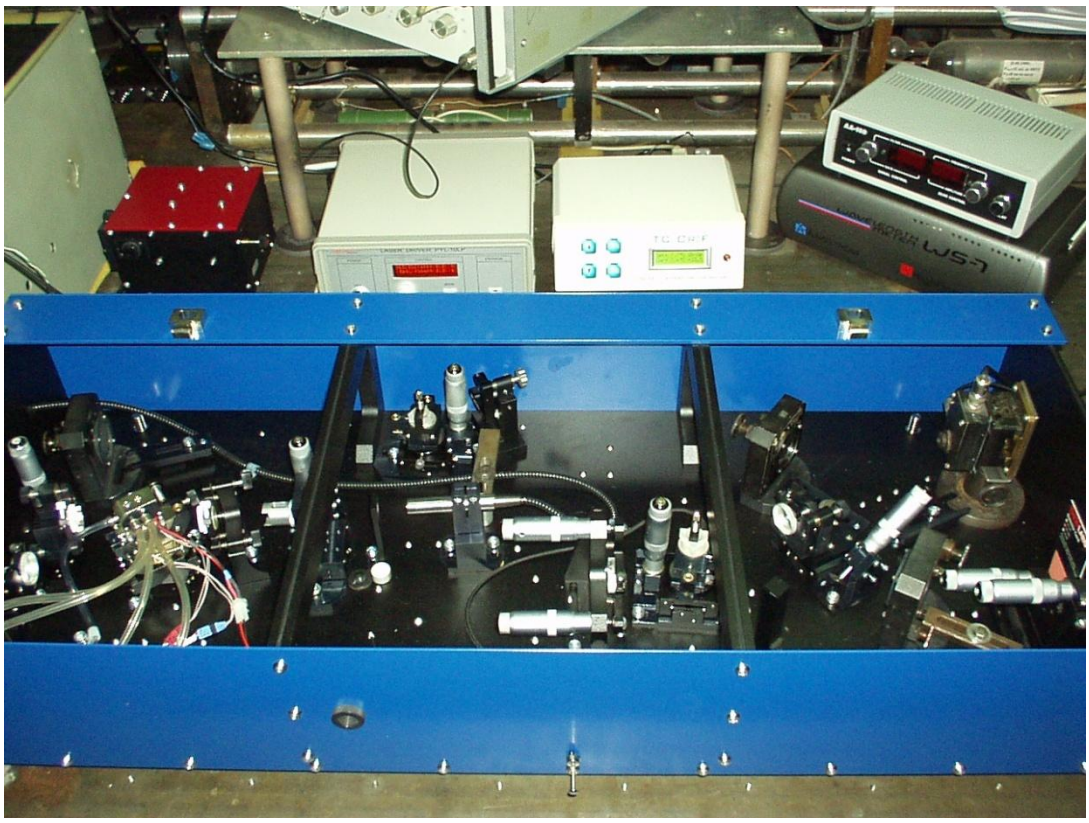

Fig. 1

The minimal cavity length and, thus, the maximal pulse repetition rate are mainly defined by the distance between prisms which, in turn, is proportional to the intracavity dispersion. Cr:Forsterite crystal has significant dispersion due to its length (10 – 15 mm). It is possible to decrease the distance between prisms by insertion in the cavity special dispersive GTI-mirrors which compensate the main part of the intracavity dispersion. The dispersion compensation with the help of GTI-mirrors allows the pulse repetition rate up to 1 GHz to be obtained. But these special GTI-mirrors are usually manufactured with quite large dispersion spread (10% and higher), so it is necessary to carefully select samples which increases the cost of laser modernization. That is why we decided to keep prisms in the cavity for fine compensation of the residual dispersion. At the higher repetition rate one needs to decrease the transmittance of the cavity output mirror in order to compensate lowering of the pulse peak power and keep KLM conditions unchanged. To improve the stability and to decrease the cavity length two concave mirrors with radii of curvature of 75 and 50 mm was used. The modified cavity has been calculated by means of a standard ABCD approach. GTI mirrors we used have the negative group velocity dispersion of –250 fs^2 per reflection. The laser can generate 40 fs pulses with average power of up to 500 mW at the repetition frequency either 100 MHz (long cavity) or 250 MHz (short cavity). Cavity configuration utilizing GTI-mirrors is shown below (Fig.2).

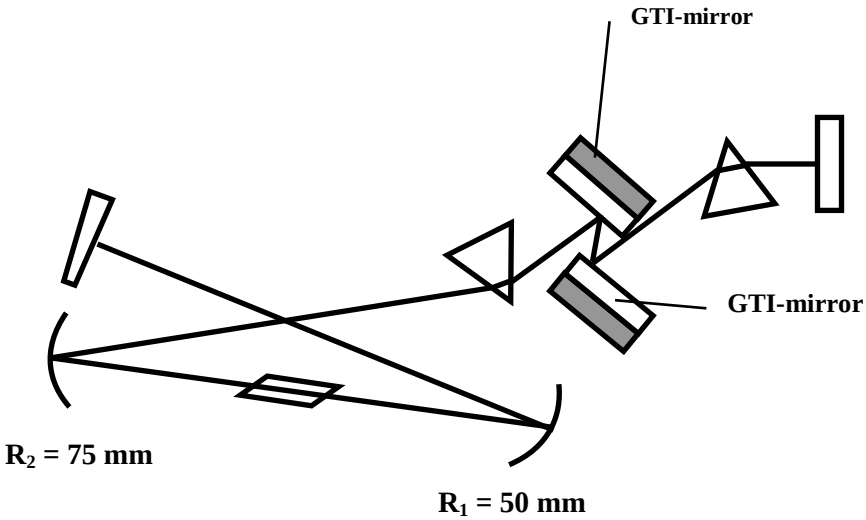

Fig. 2

A femtosecond optical frequency comb acts as a ruler in frequency space, with mode frequencies given by $f_m = m f_{rep} + f_0$, where m is an integer. The spacing of the comb modes is equal to the repetition rate of the laser, f_{rep}, which can be accurately controlled using a microwave standard. The laser pulse repetition frequency has been stabilized to the external frequency reference. H-maser having frequency stability of 10^{-14} in 100 s has been used as a RF frequency reference. The femtosecond laser cavity end mirror has been mounted on a piezo-electric transducer (PZT) to control the cavity length and thus the pulse repetition frequency. The signal at the repetition frequency has been detected at the laser output on a p-i-n photodiode with the signal-to-noise ratio of 70 dB in 100 kHz resolution bandwidth. At the first step, we have stabilized the pulse repetition frequency at 100 MHz (long laser cavity) as it is close to that of the hydrogen maser and the locking electronics does not require frequency converters to match the signal and reference frequencies.

The work on the stabilizing the 250 MHz repetition frequency also has been performed. For that signal at the repetition frequency detected at the laser output by a p-i-n photodiode has been fed to the developed phase detector where it has been filtered, down-converted and phase-compared to the reference signal at 10 MHz. The error signal proportional to the phase difference between the two signals has been sent from the phase detector to the developed high voltage amplifier and then to PZT. The repetition frequency stability has been measured to be on the order of 10^{-14} in 100 s of averaging time, thus being limited by that of the RF reference. The repetition frequency has remained phase-locked for several hours and got unlocked due to slow thermal drift of the laser cavity.

The unit has two output ports for error signals applied to PZT and EOM. The output voltage sweep for PZT is ± 300 B, and for EOM ± 100 B with DC level of 100 B. The error signals are produced in POL1 and POL2 where the reference signals synthesized from H-maser frequencies are phase-compared with the detected signals at pulse repetition (PD1) and offset (PD2) frequencies (Fig.3).

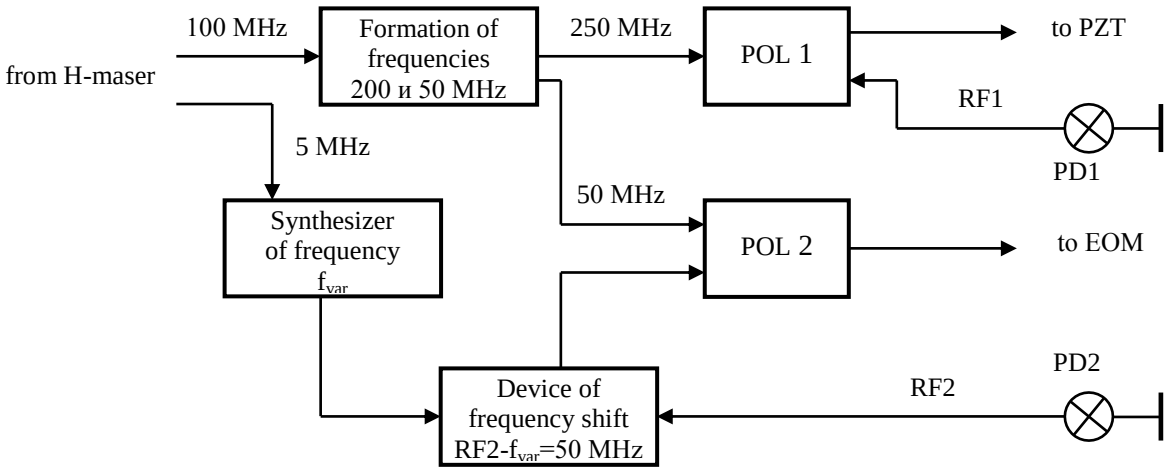

Fig. 3. Schematic diagram of the electronic control and stabilization unit for absolute and intermode frequencies of the femtosecond lasers. POL – phase offset lock system, PD – photodiode, PZT – piezotransducer, EOM – electro-optic modulator

For investigations of the Cr:Forsterite laser radiation spectral broadening few types of special HNLF fibers were produced: tapered fibers and fibers with slowly varying dispersion. It should be mentioned that both – tapered HNLF and HNLF with varying dispersion were studied for the first time. By fiber diameter changing one can vary zero dispersion length, absolute dispersion values and its slope with fixed length dependence. Dispersion variations were from 15 to –5 ps/(nm·km) for 1550 nm, while optical loss was typical as for common fibers. Three types of HNLF were investigated: fibers with constant dispersion, with slowly varying dispersion and tapered fibers.

Experimental setup is shown on Fig. 4.

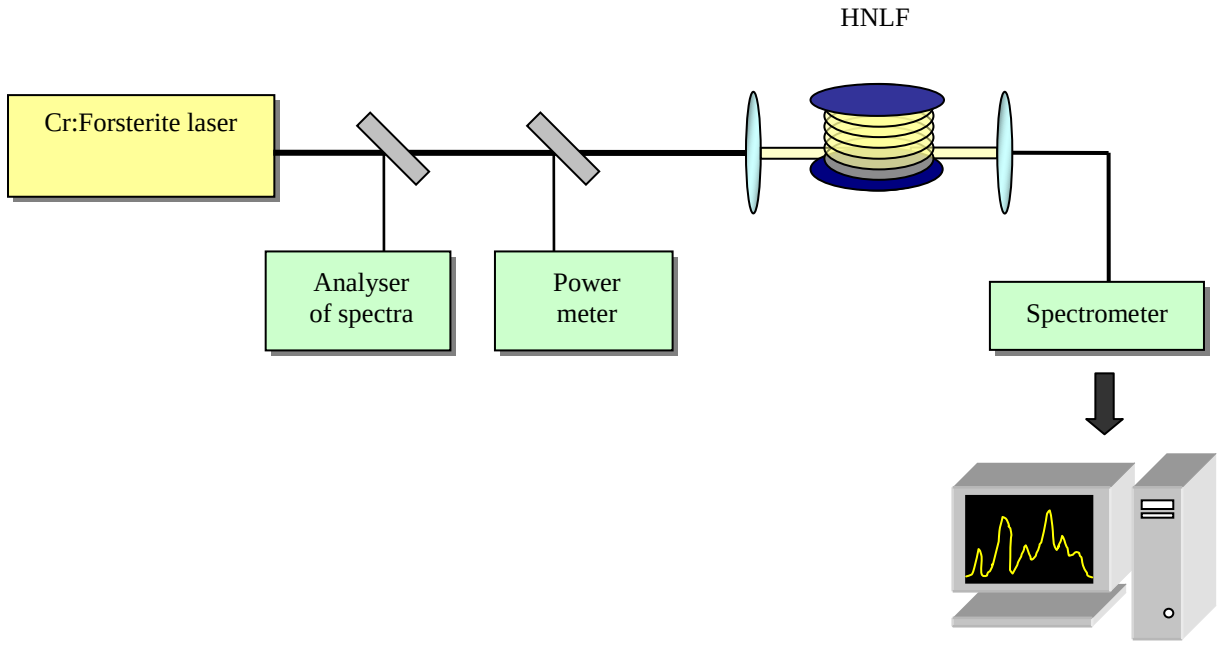

Fig. 4

The experiment was performed by use of the femtosecond Cr:Forsterite mode-locked laser, generating 40 fs pulses on central wavelength of 1260 nm, with mean power up to 500 mW and repetition rate of 100 MHz. Cr:Forsterite laser

radiation was focused in optical fiber by use of a standard 20x microlens, which was placed on the adjustment table. Pulse duration was controlled by autocorrelator. Radiation from HNLF was directed in spectrometer with resolution of 1 nm and measurement range from 1 μm to 1.8 μm. Power was registrated by measurement instrument with germanium reciever (spectral range: 800 – 1800 nm). In all experiments about 30% of laser power (~180 mW) was introduced in fiber.

Experimental Cr:Forsterite laser radiation spectrum, broadened in HNLF with constant dispersion, is shown on Fig. 5. Fiber lengths were 30 m and 50 m.
It can be seen that spectral width rise is rather low: 400 nm for 30 m fiber and 600 nm for 50 m fiber. Thus, it can be assumed that in order to reach 2 microns, fiber should be hundreds meters long. This approach is not very convenient. The better solution is to modify and optimize fiber dispersion. This can be done in tapered fiber.

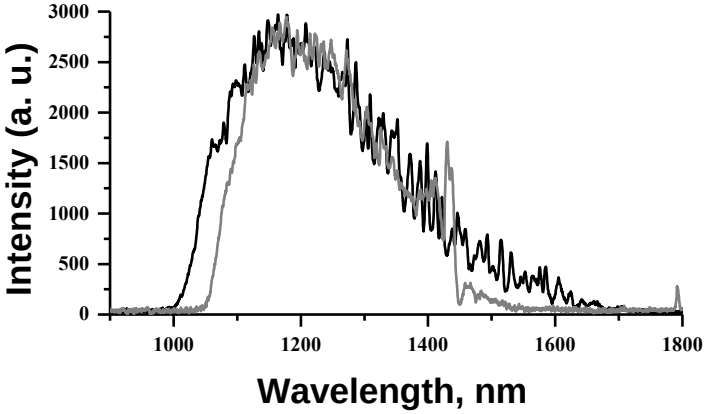

Fig. 5. Cr:Forsterite laser radiation spectrum, broadened in HNLF with constant dispersion. Black curve – 50 m fiber, grey curve – 30 m fiber.

Tapered fiber was produced from HNLF with 120 μm diameter and had a waist of 60 mm length with 2 μm diameter. Spectrum broadened in such a fiber is shown on fig. 6. It can be seen that fiber with relatively short waist (60 mm) is able to produce a spectrum of the same width as fiber of dozens meters long. This testifies much higher broadening effectiveness due to the smaller core area and also due to the zero dispersion point displacement in 1.3 μm range. According to the preliminary calculations, fiber with waist diameter less than 1.5 μm make it possible to produce a spectrum, broadened from 1 μm to 2 μm, but such fibers can be easily destructed because of high radiation intensity density, localized in waist.

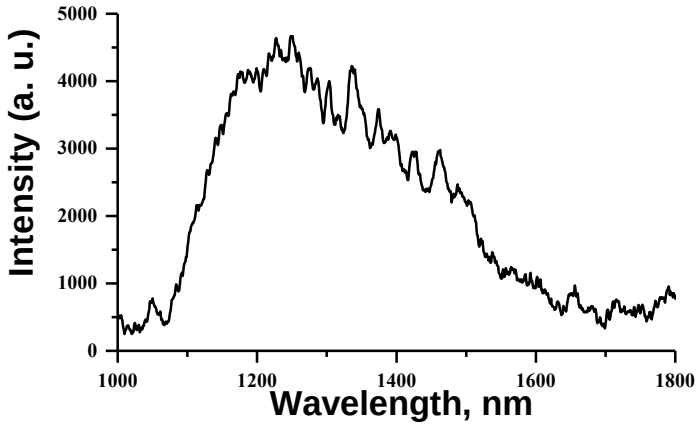

Fig. 6. Cr:Forsterite laser radiation spectrum, broadened in tapered HNLF (waist length – 60 mm, waist diameter – 2 μm).

Another way to control broadened spectrum characteristics arises when it becomes possible to vary dispersion along the fiber. This can be done by changing fiber diameter according to the specified function during fiber producing (stretching).
One of the fibers had a part with decreasing dispersion (5 meters long). Dispersion decreased linearly from 12 ps/(nm·km) to –2 ps/(nm·km) (measured for 1550 nm wavelength). Another fiber had a part with decreasing dispersion of 10 meters long and dispersion decreased from 10 ps/(nm·km) to –2 ps/(nm·km) (1550 nm). Cr:Forsterite laser radiation was introduced in the fiber butt-end with higher dispersion. Mean power in fiber was 110 mW. Experimental spectrum, broadened in such fiber is shown on fig. 7. The obtained spectrum is limited by spectrometer operating range - 1000 – 1800 nm.

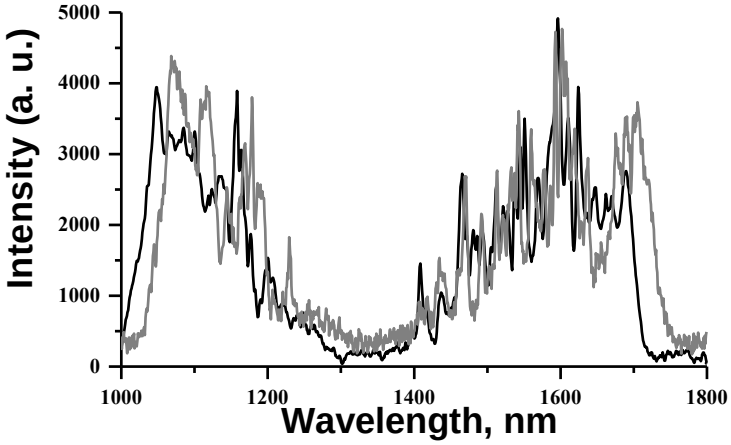

Fig. 7. Cr:Forsterite laser radiation spectrum, broadened in decreasing dispersion HNLF. Black curve – 5 meter fiber, grey – 10 meter fiber.

Spectral with for both fibers is comparable and, thus, it can be supposed that all main nonlinear optical transformations leading to spectral broadening occur in the initial part of the fiber.

In order to perform more precise measurement of long-wave spectrum edge of the signal, the simple spectrometer on the base of diffraction grating was build (stroke density is 600 str. per mm), its spectral resolution ~ 25 nm. It was shown that spectrum is broadened up to 1800 nm.

Spectral width can be increased by radiation power increasing. The dependence of spectral width from the radiation power was investigated. With the help of linear approximation the power necessary to cover one octave spectral range was estimated. For 175 mW power spectrum would be in range from 900 nm to 1800 nm. However such high power initiates a feedback, which is a Fresnel radiation reflection from the optical fiber butt-end. This feedback destroys stability of the femtosecond laser regime.

Alternatively, to cover an octave range, HNLF of higher length can be used. Silica 25 meter fiber, doped by germanium ions, was investigated. Maximum power in fiber when laser stability remained was 150 mW. Fig. 8 shows that for such fiber broadened spectrum covers an octave range (990 – 2100 nm) that allows use such spectrum to absolute frequency stabilization by means of f-2f interferometer.

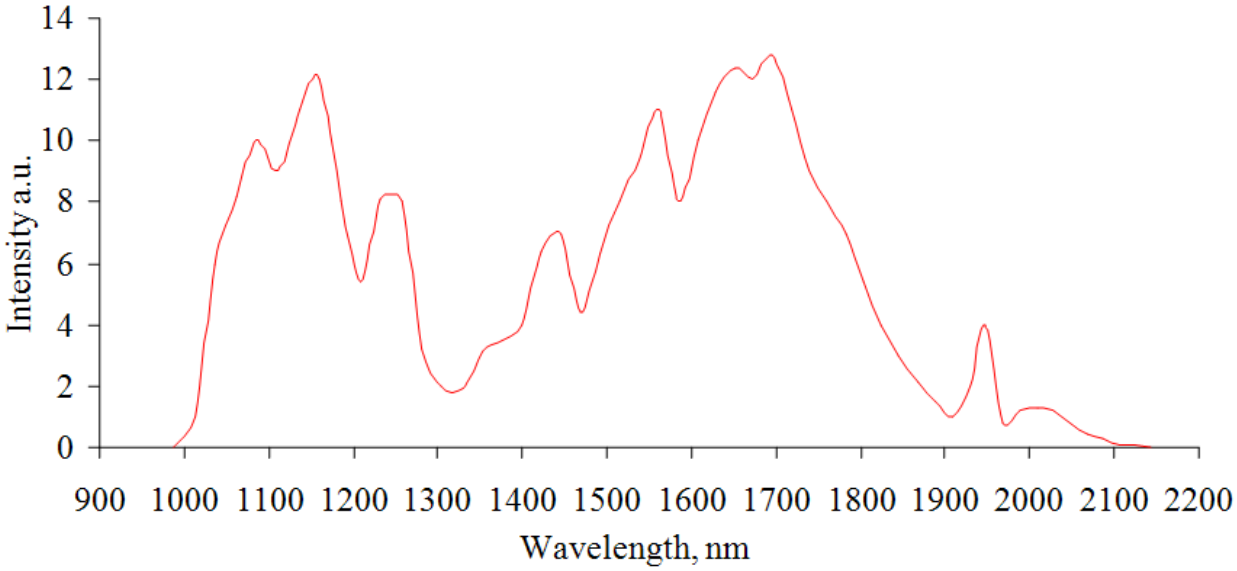

Fig. 8

Considering impressive effectiveness of supercontinuum generation technique for high-precision spectroscopy, it should be noted that spectral broadening in fibers with strong nonlinear characteristics obviously affects stability of the femtosecond frequency comb. While noise characteristics of a stationary pulse trains generated by a stable mode-locked lasers are studied theoretically perfectly, there are still a lot of questions regarding stability of the fiber outcoming radiation.

In order to study spectral changes due to the phase noise, laser radiation was modulated before HNLF fiber. Thus, radiation in fiber can be treated as a femtosecond pulse train with certain fluctuation type. Experimental measurements of spectral components relative amplitude were performed by difference frequency measurements on the fiber output by use of the radiofrequency spectral analyzer. To get more complete information these measurements were performed in different

regions of broadened spectrum along with phase modulation variations. Experimental results are presented on fig. 9.

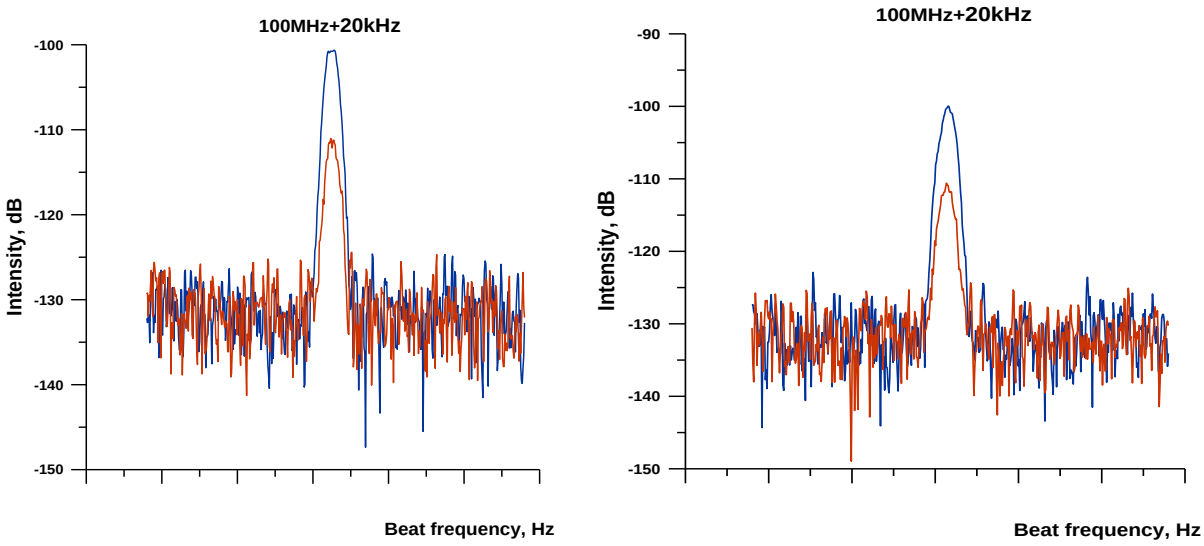

Fig. 9. Beat frequency sideband for 1 (left) and 1.25 (right) micron spectral regions of 100 nm width. Phase modulation frequency is 20 kHz.

Red and blue curves correspond to different modulation amplitudes (blue one is twice higher). Figures show that higher phase noise means higher sidebands, thus the main beat frequency component is smaller. It means that phase noise affect output spectrum and might be treated as a possible problem, since it is always essential to have a good signal-to-noise ratio. It also can be seen that sideband amplitude doesn't depend on the spectral position.

Stabilizing the Cr:F laser offset frequency (absolute frequency) has been performed by means of a nonlinear f-2f interferometer. For this the broadband supercontinuum, which has been generated in the 5-m DF-HNLF and covered one octave from 1000 nm to 2200 nm, has been employed. The long wavelength part of the supercontinuum around 2100 nm has been frequency-doubled in a 5-mm-long type-I lithium niobate nonlinear crystal. The generated second harmonic signal has been mixed with the supercontinuum part at 1050 nm to extract a radio-signal at offset frequency. Further this signal has been fed to the developed phase detector where it has been filtered, down-converted and phase-compared to the reference signal from the H-maser. The error signal proportional to the phase difference between the two signals has been sent from the phase detector to acousto-optic modulator to control the pump laser power and, thus, the femtosecond laser intracavity power and its absolute frequency (Fig.10).

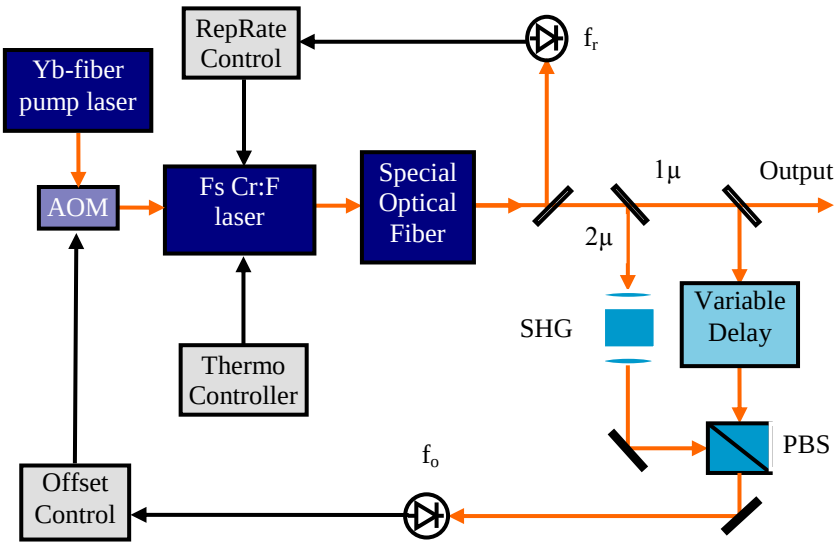

Fig. 10. Schematic diagram of f-2f interferometer

The frequency-stabilized Cr:F laser stability has been defined by comparison with the frequency of an optical standard. As an optical frequency reference we employed the 1064 nm Nd:YAG laser with the absolute frequency stability of 10^{-14} at 100 s, the laser was stabilized via its second harmonic to the R(56) 32-0 absorption line of molecular iodine. To determine the generator stability the frequency stability of a beat signal between the single-frequency Nd:YAG laser and corresponding spectral component of the broadened spectrum was measured. The beat signal frequency stability was on the order of 10^{-14} at 100 seconds of averaging time. The main stability limiting factors turned out to be the pump laser amplitude noise and the radio-frequency reference instability. On the basis of performed measurements parameters of the f-2f interferometer and locking electronics have been optimized.

An experimental setup for absolute frequency measurements of I2 lines with use of the femtosecond comb from Cr:Forsterite laser has been developed and constructed.

The schematic diagram of the setup is represented in Fig. 11. M_1, M_2, M_3, M_4, M_5 – are high reflectance mirrors; M_6, M_7, M_8 – mirrors with transmittance of ~ 50%; Gr_1, Gr_2 – diffraction gratings 600 lines/mm; Ln_1, Ln_2 – lenses; PD_1, PD_2 – Ge-photodiodes; L_1,– the cw 1064 nm Nd:YAG laser, L_2 – the cw 1030 nm Yb:YAG laser. The diffraction gratings Gr_1, Gr_2 were used to select the necessary parts of the comb spectrum at 1064 nm and 1030 nm.

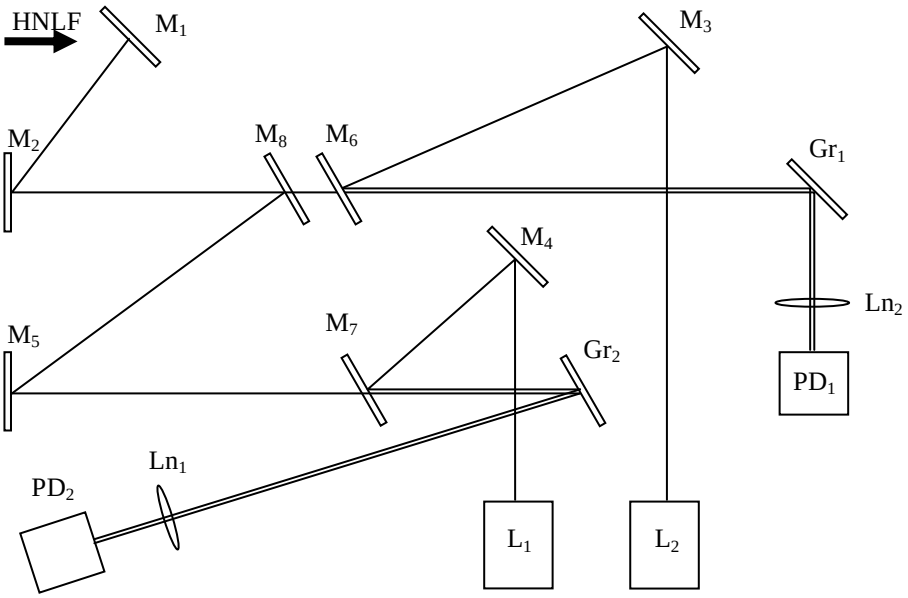

Fig. 11

The Nd:YAG laser was phase-locked to the known iodine transition at 532 nm and its frequency was known with 1 kHz accuracy. The Yb:YAG laser was, in turn, consequently phase-locked to different unknown iodine lines at 515 nm. The pulse repetition rate of the Cr:F comb was phase-locked to 100 MHz H-maser and, as the frequency of the Yb:YAG laser was pre-measured with a conventional wave-meter, the number of intermode intervals between the frequencies of the two cw lasers was calculated. Thus, having measured the frequencies of the two beat signals between cw lasers and corresponding comb components one could determine the accurate value of the Yb:YAG laser frequency and hence the frequency of the iodine transition this laser was locked to.

The frequency difference between the cw lasers L_1 and L_2 (thus the difference between known and unknown absorption lines) is given by

$$\Delta f = fL_1 - fL_2 = f_1 - f_2 + (n - m) f_{\text{rep}}$$

where f_1 and f_2 are the beat signal frequencies between the comb and the cw lasers, "n–m" is an integer, f_{rep} is the Cr:F laser repetition frequency.

The benefit of this measurement method is that there is no need in stabilization of the comb's absolute frequency (which is a complicated task) as we measure the frequency interval and it is necessary to only stabilize the comb frequency spacing (i.e. the Cr:F laser repetition rate). The beat signals were subtracted one from another to eliminate the comb components common noise.

So far we have frequency-mixed the infrared comb with the Nd:YAG laser at 1064 nm and the Yb:YAG laser at 1030 nm locked to the absorption lines of molecular iodine and obtained the beat signals at f_1 and f_2 with 30 dB signal-to-noise ratio in 100 kHz resolution bandwidth. Than these signals were mixed to produce the difference signal $|f_1 - f_2|$ which was free from the comb line common noise and this difference signal was counted with conventional frequency counter and the frequency difference between two cw lasers was calculated as the comb frequency spacing was known and the cw lasers frequencies were predetermined by wavelength measurement with a wavemeter.

3-b. Development and investigation of diode-pumped Yb-based stable femtosecond lasers

First, a two-mirror confocal cavity was used. The Yb:KGW crystal was placed in the middle between the two mirrors with radii of curvature of 50 mm. The semiconductor laser system ML500-SP with output power of up to 8W at 975 nm was used in the experiment. The output fiber had the core diameter of 200 mkm and the numerical aperture of 0.2. The pump radiation was focused into the center of the gain crystal through dichroic mirror which transmitted 80% of the pump power and less than 1% of the Yb laser power. The threshold was experimentally found to be 1.9 W in this configuration. The calculated threshold was 3 times lower. This discrepancy can be explained by non optimal pump focusing because of multimode pump beam structure. Maximal output power of the Yb laser reached 800 mW in cw mode with the transmission of output coupler of 3% and absorbed pump power of 4 W. It is possible to further increase the output power by tighter pump focusing.

Next cavity design of experimental laser we have tested was V-like geometry. Curvatures of spherical mirrors were 50 and 30 mm, one of those was dichroic. The pump was focused into the crystal through this dichroic mirror by a 35 mm lens. In the experiment a 10-at. % Yb3+-doped KYW crystal cut along c-axis was used. The length of crystal was 1.6 mm. The semiconductor laser system ML500-SP with output power of up to 8W was used in the experiment. Parts of the laser radiation were directed to RF and optical spectrum analyzers to register the intermode beats and optical spectrum width respectively. Spectrum analyzer «Rohde&Schwarz» for radio range and spectrum analyzer «Ocean Optics» for optical range were used. For measurement of pulse duration an autocorrelator was used. We had not found any information about dispersion of the Yb:KYW crystal in publications and this fact had make enough difficulties for us. It is only possible to estimate dispersion of crystal as about 1000 fs^2/mm. During an extended research we could not obtain stable KLM operation.

For the next stage we decided to use a semiconductor saturable mirror (SESAM) from «BATOP GmbH» with 2% variation of the reflection index at 1.045mkm. As the result of investigation a femtosecond operation was achieved, but it was rather unstable.

We have deducted that the use of pump source with multimode fiber output is not appropriate. We have made decision to purchase a recently emerged on the market 3-W serial pump source from «Unique-mode». A beam of this source has divergence about 10 times more then diffractive divergence. As we estimate this pump source can fulfill designed requirements. The pump laser generates up to 3 W at the wavelength of 980 nm. Dependencies of output wavelength on the current at 25°C are shown on fig.12. It is possible to choose optimal pump wavelength by means of varying temperature and pump current.

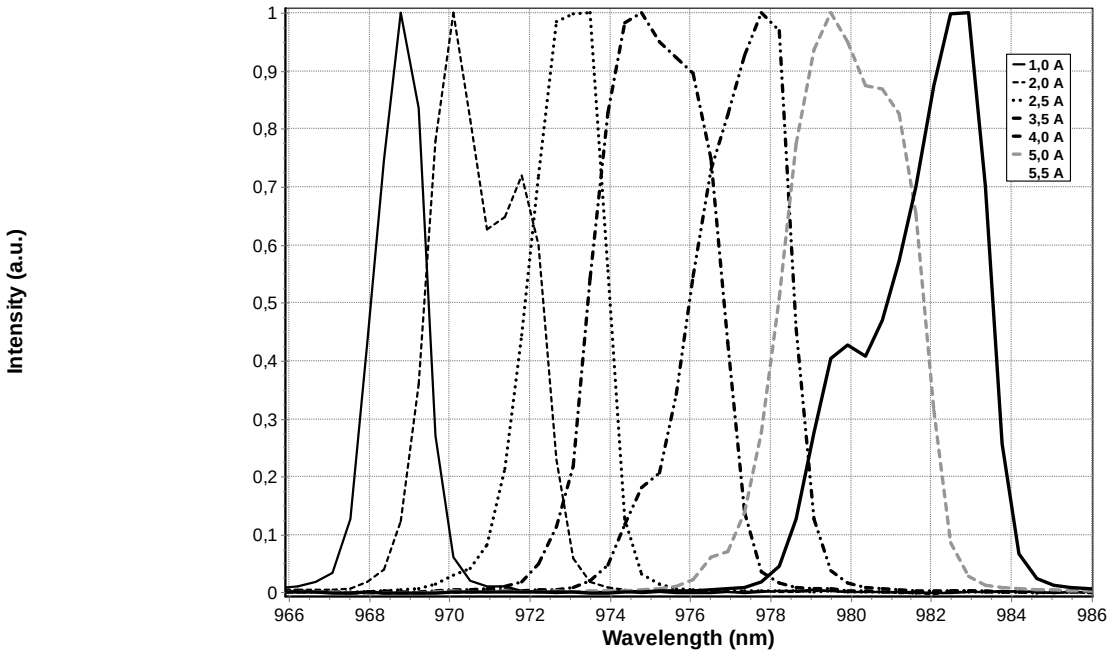

Fig. 12

The pump radiation is linearly polarized and has the beam quality parameter $M^2_x \sim M^2_y < 10$. The pump laser module and the developed power supply and thermo-controller are shown in fig. 13. We don't know any published works in which femtosecond operation of Yb-based laser with 300-500 MHz repetition rate using this pump source was described.

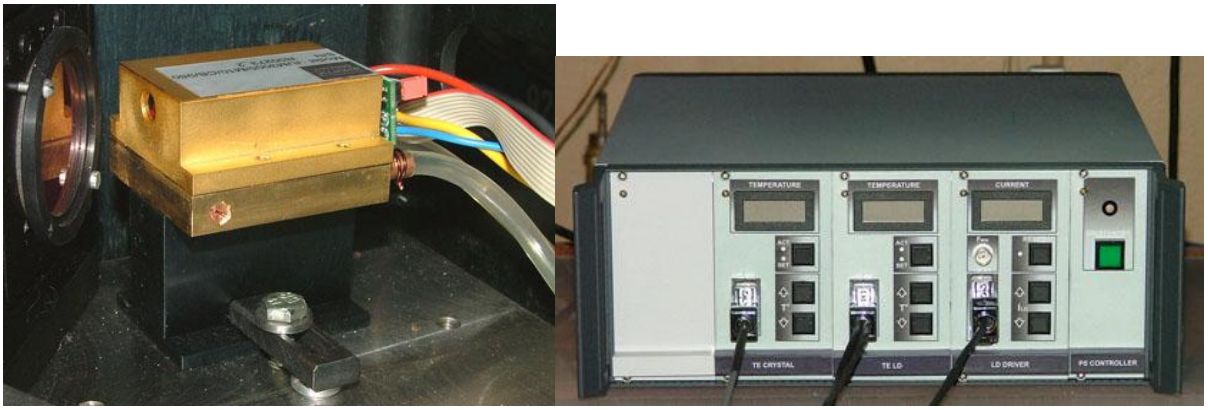

Fig. 13. Pump laser module (at left), developed power supply and thermo-controller (at right).

Initially the Yb:KYW laser cavity has been assembled in classical X-configuration with the dispersion compensation by means of two Brewster-cut prisms (Fig.14). The active crystal has been cooled down to 15°C with the help of a thermo-electric cooler. The lasing threshold is 0.5 W of the absorbed pump power. The output power of 800 mW at the absorbed 2.3 W of pump (which means the laser slope efficiency of 61%) has been obtained in the cavity without prisms. After the prisms insertion the output power has been 230 mW at the same pump level (slope efficiency ~ 18%). The output power stability was not worse than 0.1%, comparing to 5% when pumped by a multimode-fiber-coupled laser. Because of no any data for dispersion of used crystal in publications, for

establishment of femtosecond operation it is needed to experimentally find the range between prisms, working point at stability range and value of pump power. Only if all of these parameters precisely selected stable femtosecond regime can be obtained. It is quite labor-consuming work. In addition it is known from publications that femtosecond operation of Yb-based laser without nonlinear semiconductor mirror (SESAM) exists only in enough narrow range of parameters values.

Fig. 14

We used conventional X-like resonator geometry (fig.15). Range between prisms (SF8 glass) was changed in bounds 20 – 45 cm. Pump power was varied from threshold value up to maximal value (3 W). Working point was tried at slopes of both stability regions. Semiconductor mirror with modulation depth 2% (BATOP) was used. Occurrence of femtosecond regime or closeness to the one was controlled by oscilloscope, optical spectrometer and radio frequency spectral analyzer. Approximate operating parameters were estimated, but stable mode-locked regime was not obtained.

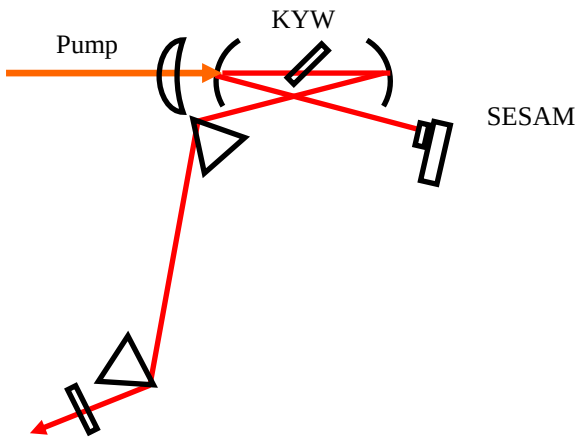

Fig. 15

From calculations follows that intermode frequency of laser with prisms is less than 200 MHz. But for our aims i.e. for building of femtosecond optical clocks and frequency synthesizers of wide application it is needed to have intermode frequency in 300 – 500 MHz range. Usage of spherical mirrors with smaller ROC for resonator length decreasing (therefore increasing of intermode frequency) is unacceptable due to constructive restrictions. It is apparently the big range between prisms gives general contribution to resonator length. Therefore we have decided to compensate major part of dispersion by GTI mirrors which recently commercially available in Layertec company. Such mirrors where bought. They have dispersion about $-1000 fs^2$ per reflection and compensate major part of active medium dispersion. Proposed resonator design using GTI is shown on figure 16. Prisms are used for accurate dispersion tuning because of the GTI have variation of parameters value up to 10% and its dispersion depends on beam incident angle. Such design allows us to achieve intermode frequency more than 300 MHz.

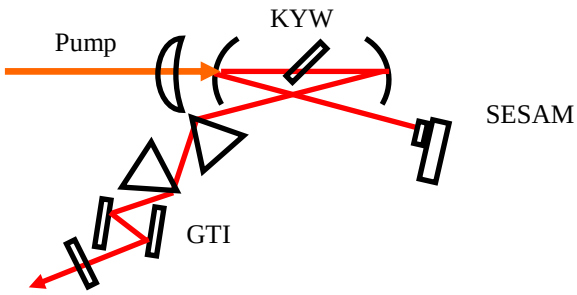

Fig. 16

Range between prisms was varied in range 0 – 20 cm, pump power was changed from threshold value to maximal allowed power (3 W). Resonator was adjusted in such manner that operating point lied on edge of stability range. Both of resonator stability ranges were studied. Existence of mode-locked regime or approaching to the one was controlled by high frequency oscilloscope and radio frequency spectrum analyzer. Typical time dependence of radiation intensity is shown on figure 17. Modulation period was varied from 10 to 100 μs depending on pump power and focusing on the SESAM. This is typical Q-switching due to saturable element in resonator, in our case it is SESAM. Growing of focused beam size on the SESAM we obtain continuous generation without mode-locking because of SESAM stops saturating. Figure 17 shows on of pulses with time resolution about 5 ns. Beats of some modes can be seeing.

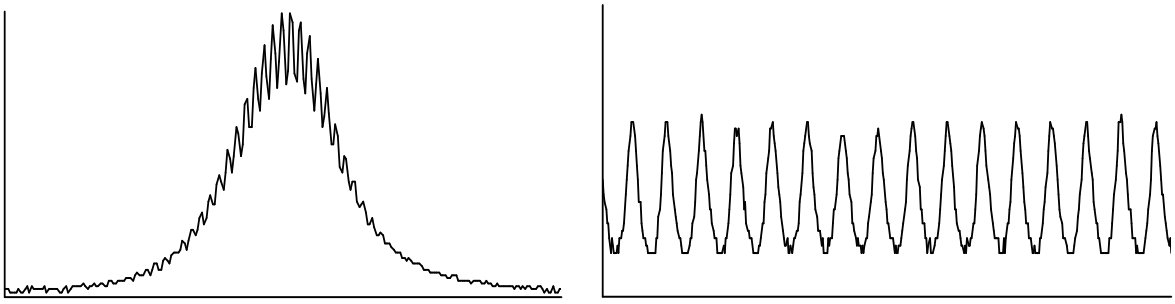

Fig. 17

So from fig. 17 we can conclude that non stationary generation (pulsing) does not allow to mode-locked regime to be established. In similar works when repetition rate about 100 MHz or/and pump source with diffractive divergence at least in one plane is used stable mode-locked operation is achieved. It seems that in our case one of the reasons of instability is the impossibility of focusing of pump beam in crystal inside the laser mode waist size. To check this it is planned to investigate the mode-locked regime with available pump source and at pulses repetition rate about 100MHz. At this condition it is possible to obtain required pump focusing.

3-c. Investigation of the process of spectrum broadening of Cr:Forsterite femtosecond laser highly nonlinear fibers

Theoretical Model Description

Since femtosecond laser radiation appears to be a femtosecond pulse train, let us consider a femtosecond pulse train after propagation through a fiber in the following form:

$$F(t) = \sum_n f_n(t - nT_0) \qquad \text{(T1)}$$

Here T_0 is an interpulse time and $f_n(...)$ - n-th pulse shape, that can be found as a numerical solution of nonlinear Schrödinger equation (NLSE) [1]:

$$\frac{\partial f}{\partial z} = \hat{D}f + \frac{i}{L_{NL}}|f|^2 f \qquad \text{(T2)}$$

where $\hat{D} = \sum_{m=2} \beta_m \frac{i^{m+1}}{m!}\frac{\partial^m}{\partial t^m}$ is a dispersion operator, β_m - group velocity dispersion (GVD) of the m-th order; $L_{NL} = \gamma P_0^{-1}$ - nonlinear length; γ - parameter of nonlinearity related to the effective mode area; P_0 is the pulse peak power.

In this paper we concentrate on SPM and dispersion as a main effects, assuming that except SPM no other nonlinear effects, such as self-steepening or stimulated Raman scattering, take place. Numerical calculation of the NLSE (T2) can be performed by self-split Fourier method (SSFM).

If pulse train (T1) is perfect, which means that it is assembled with pulses of equal parameters, its power spectrum can be expressed [2] as a combination of discrete spectrum (femtosecond comb) and envelope:

$$P(\omega) = |F(\omega)|^2 H(\omega T_0), \qquad \text{(T3)}$$

where $F(\omega) = \int_{-\infty}^{\infty} f(t)\exp(i\omega t)dt$, $H(\omega T_0) = \frac{1}{2N_p+1}\left|\frac{\sin\left[\frac{1}{2}(2N_p+1)\omega T_0\right]}{\sin\left(\frac{\omega T_0}{2}\right)}\right|^2$ - discrete spectrum of finite pulse train.

In the presence of fluctuations both spectral envelope and discrete spectrum undergo changes, that can be estimated numerically.

Thus, we can divide the general problem of femtosecond pulse broadening into two parts: first is perfect pulse train broadening, when the pulse train spectral envelope coincide with a single pulse, and the second – spectral broadening of noisy train.

The first problem can be calculated directly by use of NLSE.

Numerical model in presence of noise consists of the following stages. First, we calculate propagation through a fiber of N_p pulses with random intensities in a given range. Then we assemble a pulse train as a time series of a form (T1). And the last stage is calculation and comparison of perfect and perturbed pulse train spectra.

Numerical calculation of Spectral Broadening in HNLF: pulse propagation in HNLF DDF

Numerical modeling of the pulse propagation problem in highly nonlinear optical fibers with decreasing dispersion differs from the one, describing pulse evolution in common fibers. While for common optical fibers nonlinear and dispersion characteristics usually remain the same along the propagating distance, diameter variations in decreasing dispersion HNLF lead to variations both in dispersion profile and nonlinear coefficient (via effective area A_i^{eff}): $\gamma_i = n_2\omega_0 / cA_i^{eff}$, which means that in each point on a propagation distance nonlinear and dispersion lengths are unique.

Though, the most valuable difference is due to dispersion variances. Dispersion profile in each fiber point can be estimated by profile with correspondent fiber diameter (see Fig.18.).

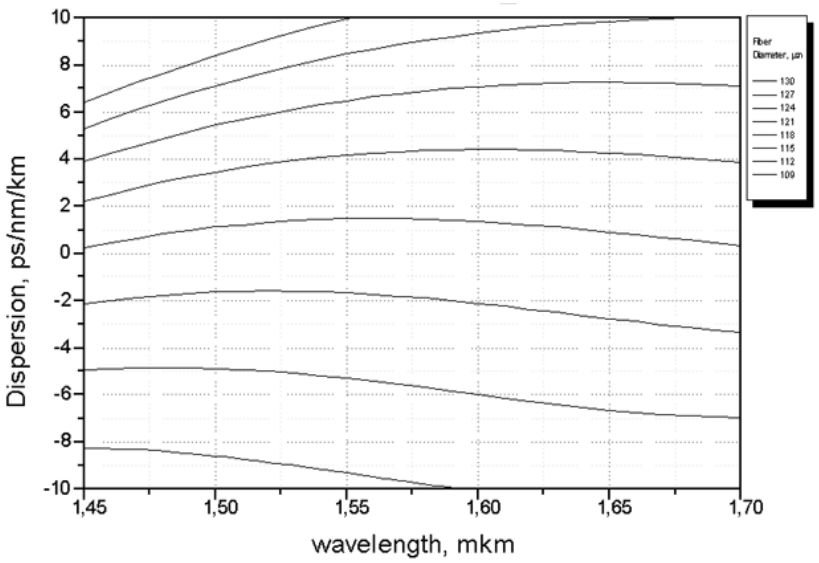

Fig. 18. Dispersion profiles of HNLF with different diameters.

In these circumstances it is impossible to use general nonlinear Schrödinger equation and self-split Fourier method with fixed and stable parameters. In order to consider dispersion and nonlinear variations perfectly it is necessary to solve NLSE for each spatial step with its unique parameters separately.

$$\frac{\partial A}{\partial z} = \left(\hat{D}_i + \hat{N}_i\right) A \qquad \text{(T4)}$$

$$\hat{N}_i = i\gamma_i \left[|A|^2 A + \frac{2i}{\omega_0} \frac{\partial}{\partial t} \left(|A|^2 A \right) - T_R A \frac{\partial}{\partial t} |A|^2 \right]$$

$$\hat{D}_i = -\frac{i}{2} \beta_{2i} \frac{\partial^2 A}{\partial T^2} + \frac{1}{6} \beta_{3i} \frac{\partial^3 A}{\partial T^3} - \ldots,$$

here we assume that β_{2i} - group velocity dispersion for the *i-th* integration step, i.e. GVD for the *i-th* fiber point which can be estimated as a GVD of HNLF fiber with equal diameter. GVD of higher orders and nonlinear coefficient γ_i can be estimated the same way.

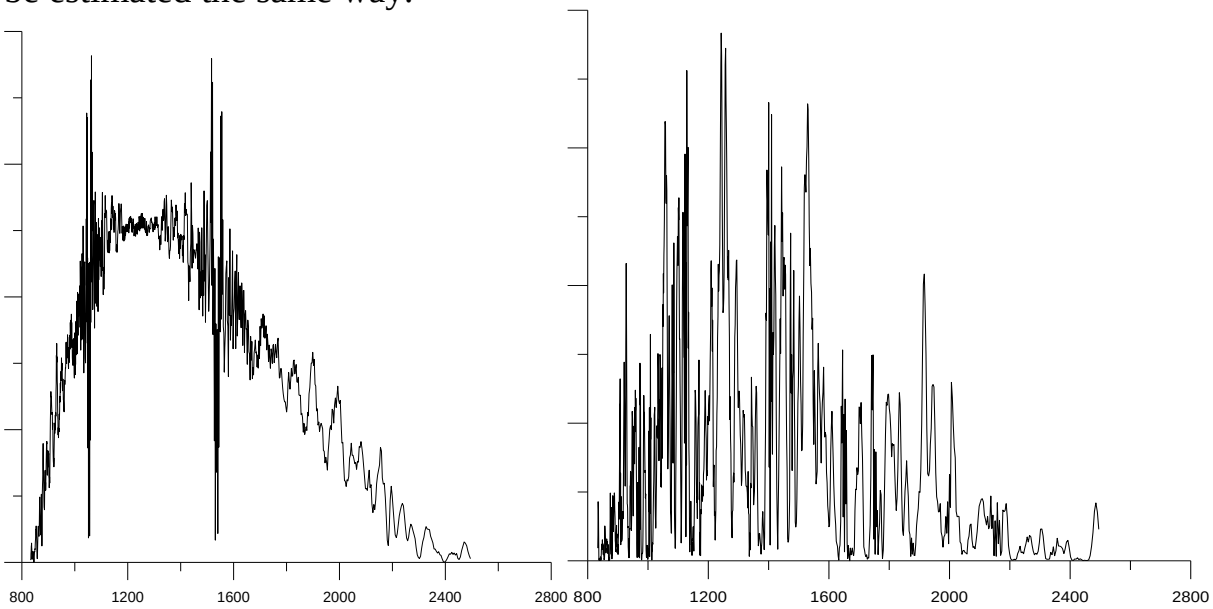

a) P=120mW, D~145--150, L=10m b) P=120mW, D=133--113, L=20 m

Fig. 19. Broadened pulse spectra after propagation in HNLF of different configuration.

Calculation results of pulse spectrum after propagation in HNLF for two different fibers is presented on Fig. 19.

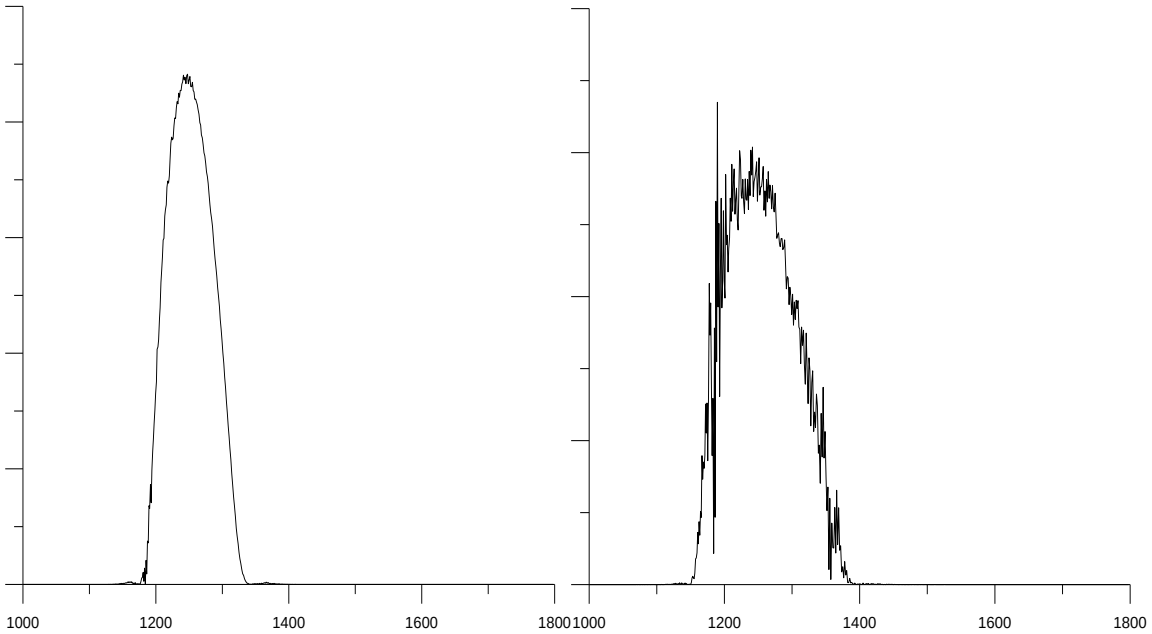

a) L=1 m b) L=2 m

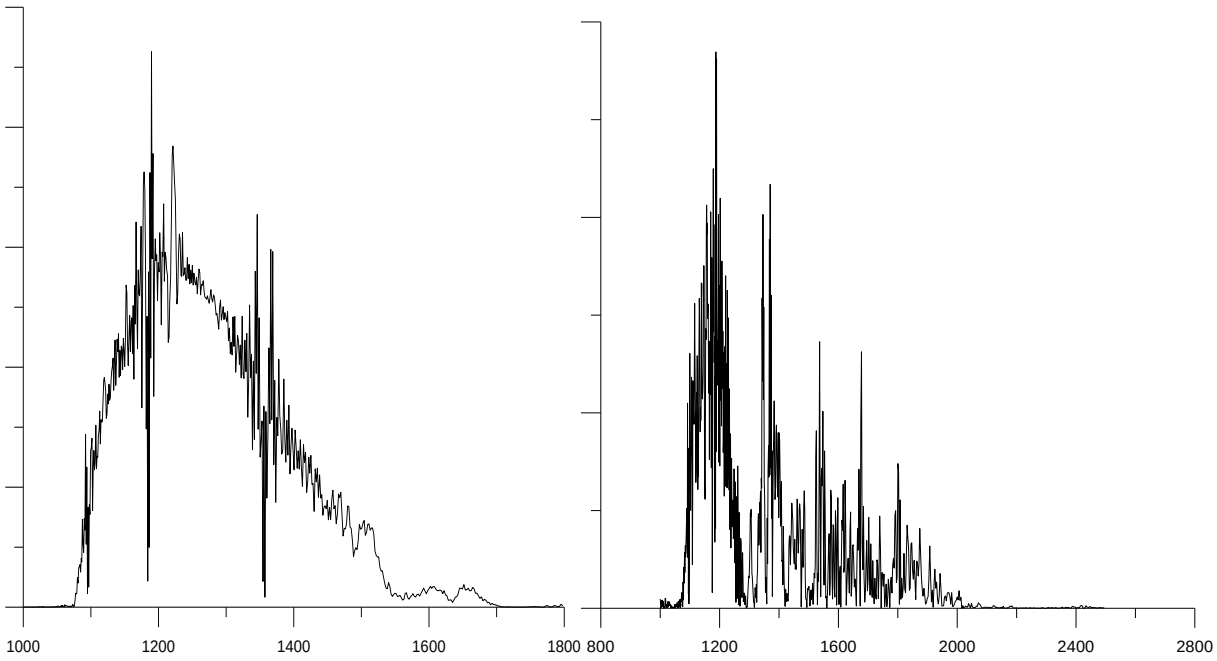

c) L=5 m d) L=15 m

Figure 20. Spectral evolution, calculated for a 40 fs pulse, propagating in HNLF. Laser power 120 mW. Fiber diameter varies from 130 to 145 mkm. a-b-c-d pulse location (propagated length)

Fig 20. shows spectral evolution in one fiber. It can be seen that spectral broadening especially effective on the first meters.

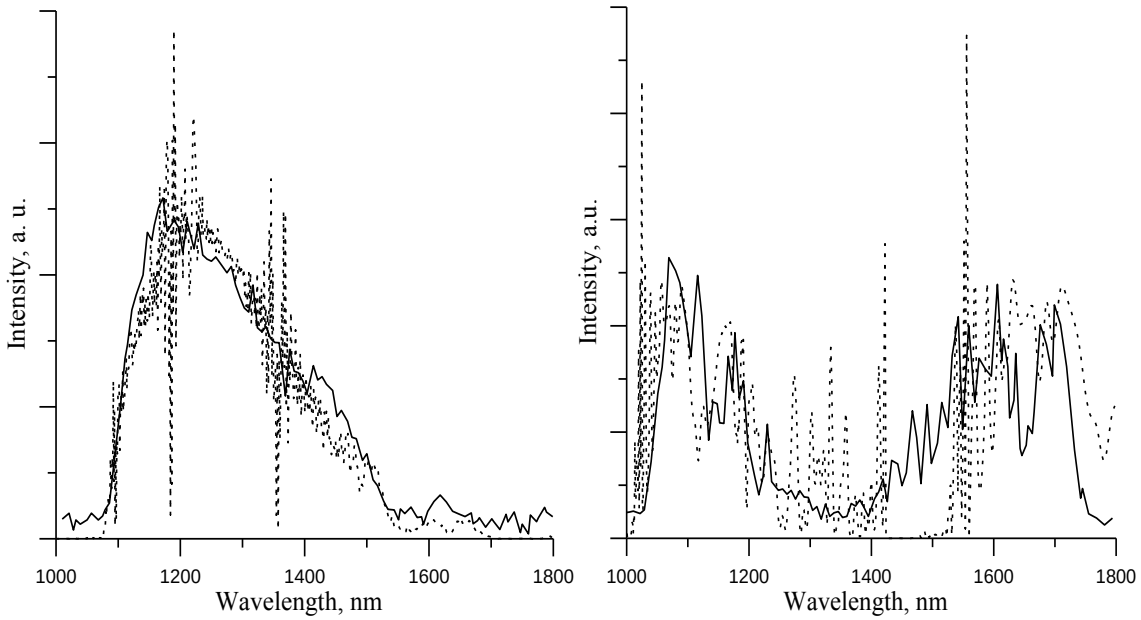

Fig. 20d. Comparison with experiment. The Cr:F laser spectrum broadening in 7-m long HNLF DDF, dashed lines – simulated spectra, solid lines – experimental spectra. The light enters the fiber from the end with dispersion parameter of -13.8 ps/nm*km (left graph) and -6.6 ps/nm*km (right graph).

Generally, there are three ways to increase spectrum width:

1. To increase laser radiation power.

Since nonlinear spectral broadening in optical fibers is nonlinear effect, radiation power is the main factor, determining spectral width, however it should always be considered along with other fiber and radiation parameters.

2. To use longer fibers.

Fiber length is important while pulse peak power is great enough to provide noticeable spectral broadening. While during propagation pulse duration increases due to dispersion influence, peak power reduces, which means that nonlinear effects get less effective. Thus, for HNLF fibers with average power of about 100 mW, fiber length should not be greater than 20-30 meters, since the main spectral broadening happens on the first 5-10 meters and further it rises insignificantly. Thus, it is defensible to use long fibers if laser source power is small.

3. Make fiber parameters optimal.

Among the fiber parameters that can be optimized in order to get the widest spectrum, nonlinear coefficient and dispersion should be mentioned in the first term. First, it is possible to increase nonlinear coefficient γ. Usually this can be done by doping. This acts the same way as in the case of increasing radiation power, since both methods lead to decreasing nonlinear length and nonlinear effects became more influent. The second method is to reduce dispersion. It is especially important to get the smallest GVD β_2 on the fiber input, where pulse duration is small and peak power is the highest. It should be noted that spatial dispersion profile is also very important for spectrum shape.

Model of tunable laser radiation broadening in HNLF

Here we'll discuss the situation, when laser radiation wavelength is varying while fiber remains the same.

The only difference in this case is in dispersion profile interval covered by pulse spectrum. If laser is tunable, it can be tuned on the zero dispersion wavelength, as well as on the other places, where the dispersion absolute value might be high. Figure 21 shows broadened spectra of three pulses with equal power and shapes, but different central frequencies. The blue curve corresponds to the case when central wavelength is close to the zero dispersion point, green and red curves have noticeable absolute dispersion values, the red curve has greater dispersion than the green one. It can be seen that the higher dispersion is, the less spectral broadening occurs. It is a pretty clear result since dispersion always prevents spectral broadening.

Figures 22 and 23 show spectra, depending on the pulse power. It can be seen that for high absolute dispersion values spectral broadening is small and remains practically the same, while radiation power gets three times higher. The opposite case can be observed on figure 3, where absolute dispersion value is low and spectral broadening is very sensitive to the radiation power.

For the HNLF DDF with varying dispersion we have some kind of mixture of these cases. However it is a much more complex calculation problem, since highly nonlinear fibers with varying dispersion are very inconvinient objects for a dispersion profile and raman parameters determination. These parameters are individual for each fiber point and thus can't be measured directly. To solve a propagation problem many characteristics should be approximated, for example we considered that dispersion change along the fiber length was linear. Small values of high order dispersion (which is typical for HNLF) permit in some way to minimize possible errors.

For a thorough raman scattering calculation it is necessary to know a fiber raman response function. Unfortunately, for the fibers we used in investigations, there were no experiments to find raman parameters because of complex fiber geometry. In calculation we used typical fiber raman parameters. Numerical investigation also show that the results (broadened spectra) are more sensitive to the dispersion and nonlinear parameters, than to the raman variations. In other words, it is laser power and dispersion profile that are most critical both for the value of spectral broadening and for the spectral shape.

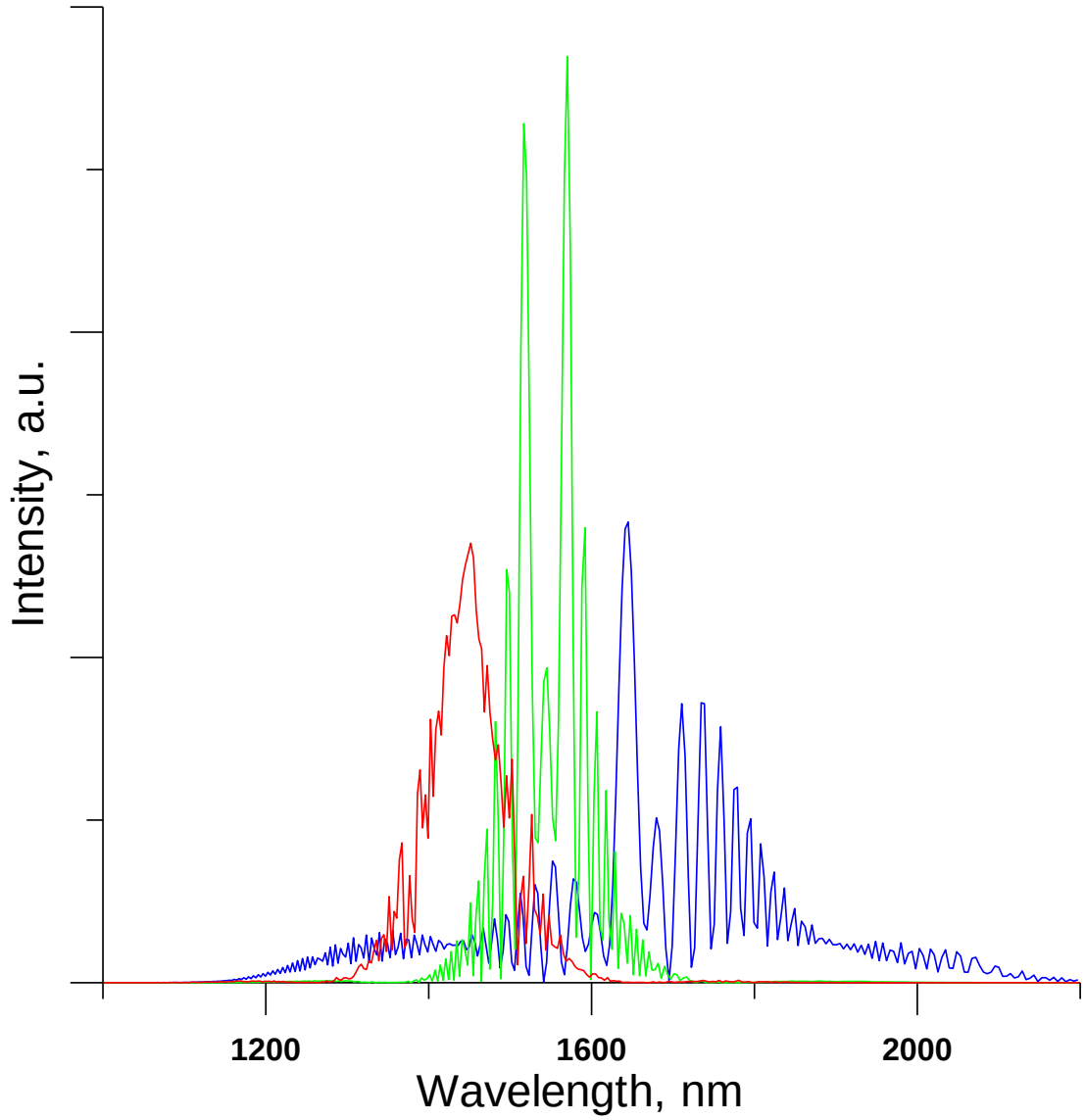

Figure 21. Three pulses of equal shapes and power broadened in the same fiber. Central wavelengths: blue – 1560 nm ($\beta_2 = -0.2\ ^{ps^2}/_{km}$), green 1460 nm ($\beta_2 = -5\ ^{ps^2}/_{km}$), red – 1360 nm ($\beta_2 = -20\ ^{ps^2}/_{km}$).

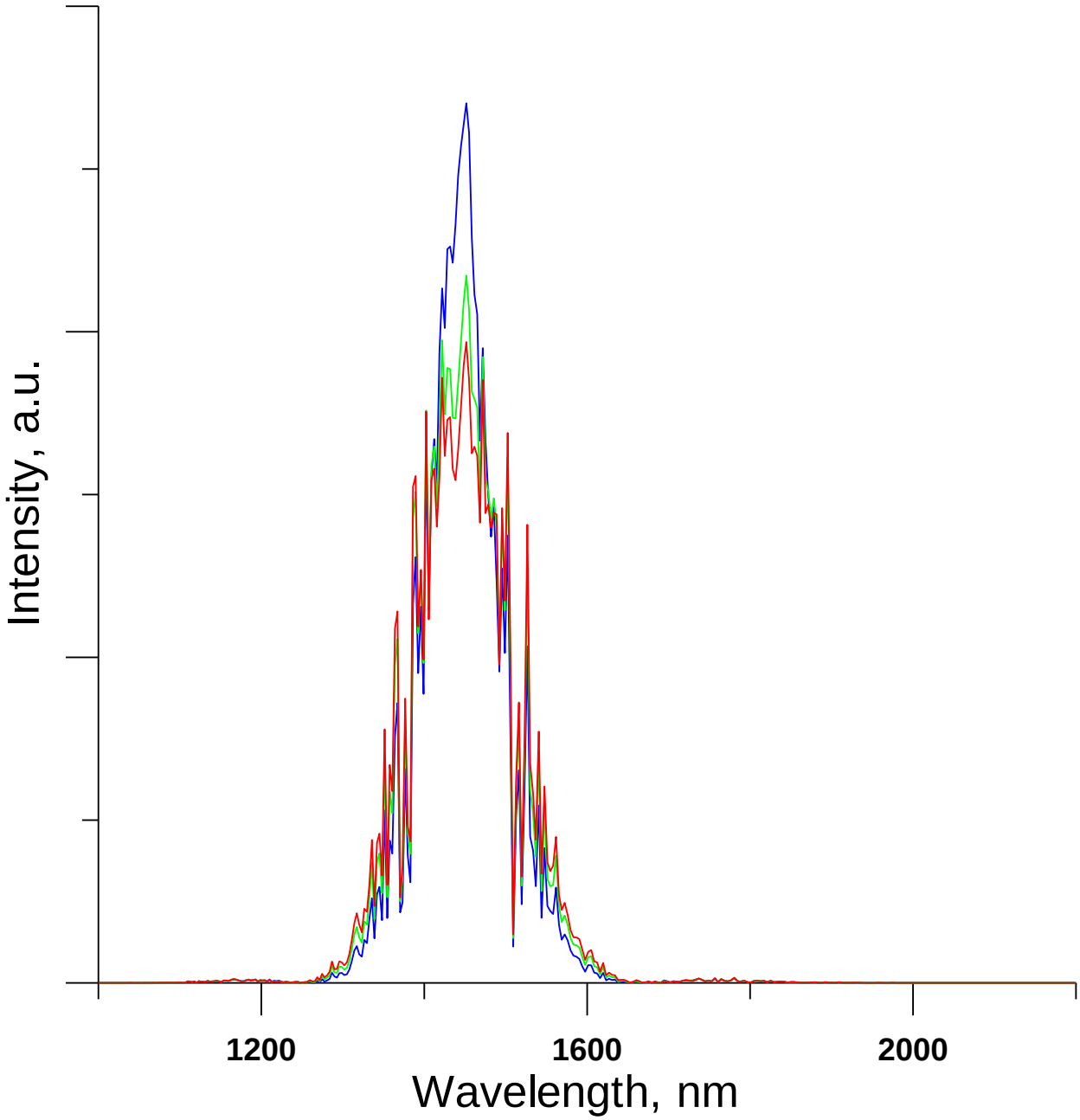

Figure 22 Spectral broadening with high absolute dispersion value. Laser power: blue – 30 mW, green – 60 mW, red – 90 mW. Central wavelength - 1360 nm ($\beta_2 = -20\ ^{ps^2}/_{km}$)

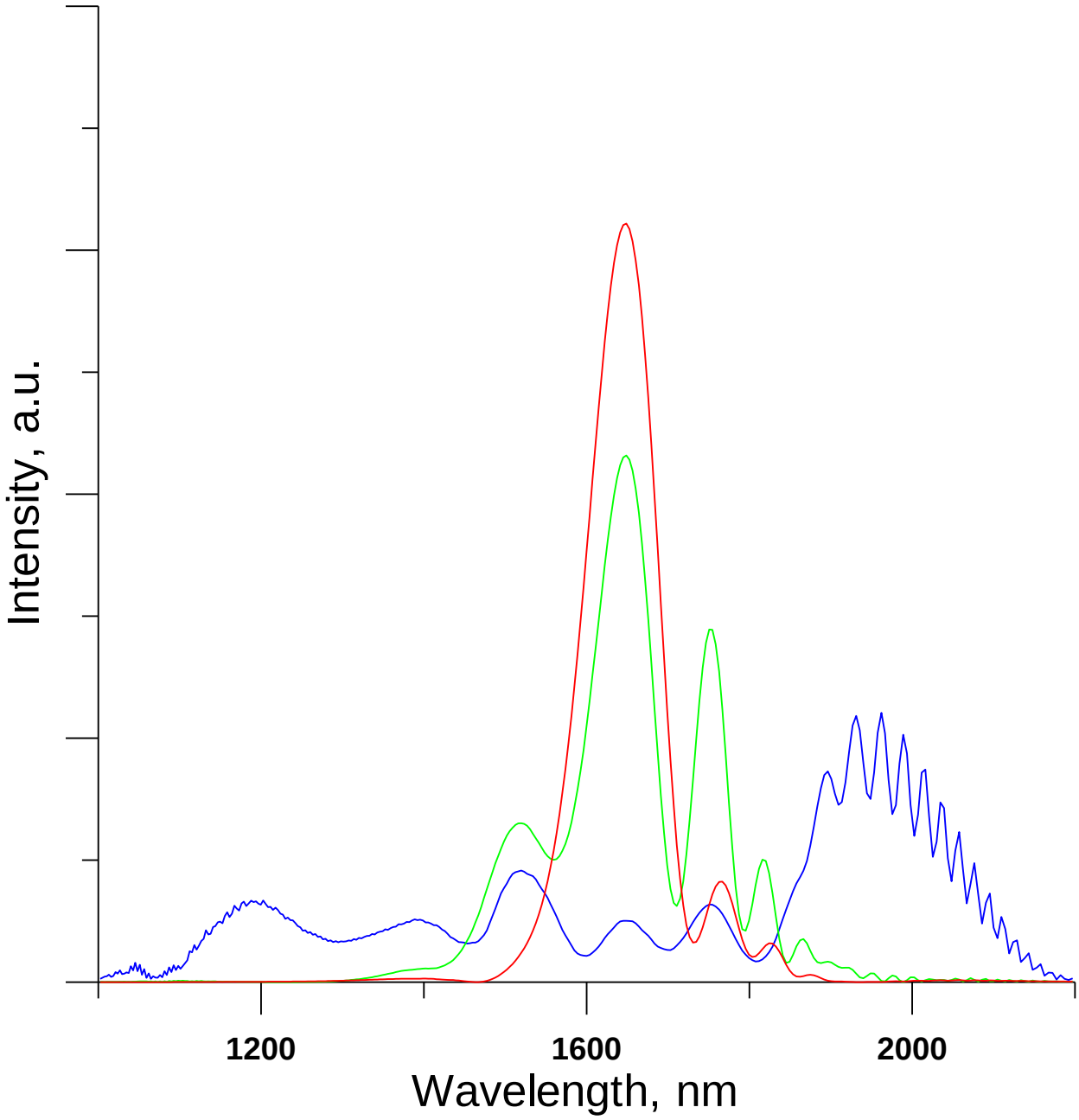

Figure 23 Spectral broadening with low absolute dispersion value. Laser power: blue – 90 mW, green – 60 mW, red – 30 mW. Central wavelength - 1360 nm ($\beta_2 = -0.2\ ^{ps^2}/_{km}$)

Pulse Train Noise in Fibers

Intensity noise and self-phase modulation in HNLF

Self-phase modulation (SPM) is the main reason of spectral broadening in highly nonlinear fibers SPM, since intensity in fiber is extremely high and fiber length is usually shorter or comparable to the dispersion length. While it is not the only effect driving spectral evolution, in first approximation for the simplicity we exclude the others. The solution of the nonlinear Schrodinger equation - temporal

profile of the broadened pulse shape, which is determined by nonlinear phase $\varphi(T)$, caused by SPM is determined as:

$$f(t) = f(0)\exp(i\varphi) \qquad \text{(T5)}$$

$$\varphi(T) = \left|f(0,T)\right|^2 \xi, \qquad \xi = \frac{z_{eff}}{L_{NL}} \qquad \text{(T6)}$$

This presentation is valid for the case when no other than SPM nonlinear or dispersion effects affect the pulse spectrum.

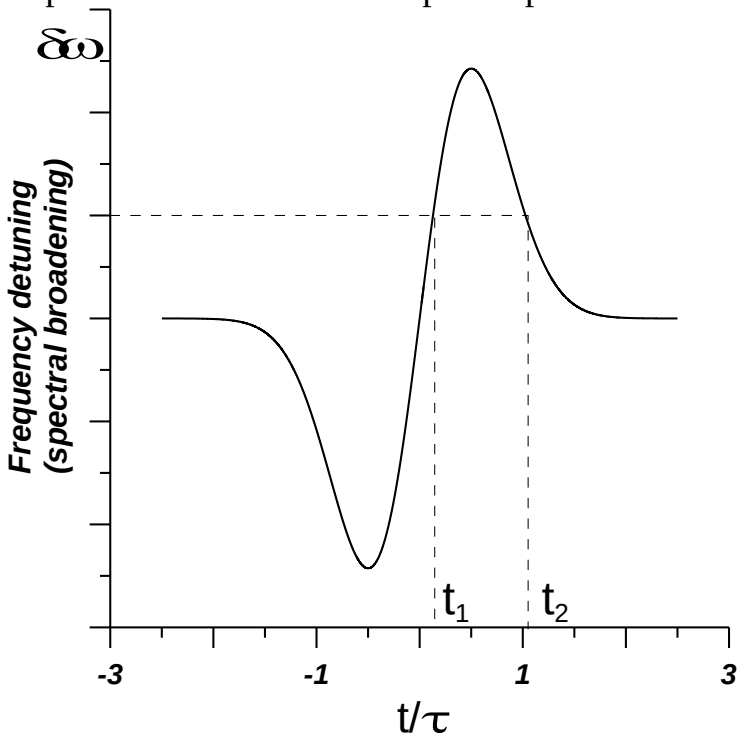

Figure 24. Spectral broadening by SPM. For all frequencies except maximal and minimal, on pulse temporal profile there are two points (t_1 and t_2) with equal detuning from the central frequency.

Let us consider a train of pulses with equal shapes and random intensities. Since nonlinear phase is sensitive to pulse amplitude, random intensity lead to random phases in all pulse points. Thus, if $\xi = 10^3$, $\partial\xi/\xi = 10^{-2}$, then phase differences for a certain frequency within the pulse train can be estimated as $\Delta\varphi(T) = \left|f(0,T)\right|^2 \delta\xi \le 10$, i.e. for the most part of the spectrum of a train with intensity stability of about 10^{-2}, phase uncertainty exceeds π. This means that one spectral component can be in maximum or in minimum for different pulses.

Figure 25 show broadened spectra of Gaussian pulse trains with intensity fluctuations after propagation in fiber with strong self-phase modulation, calculated for a trains with 10^3 pulses. Qualitative estimations show that 1-10% intensity stability and thus - nonlinear phase uncertainty leads to considerable spectral distortions.

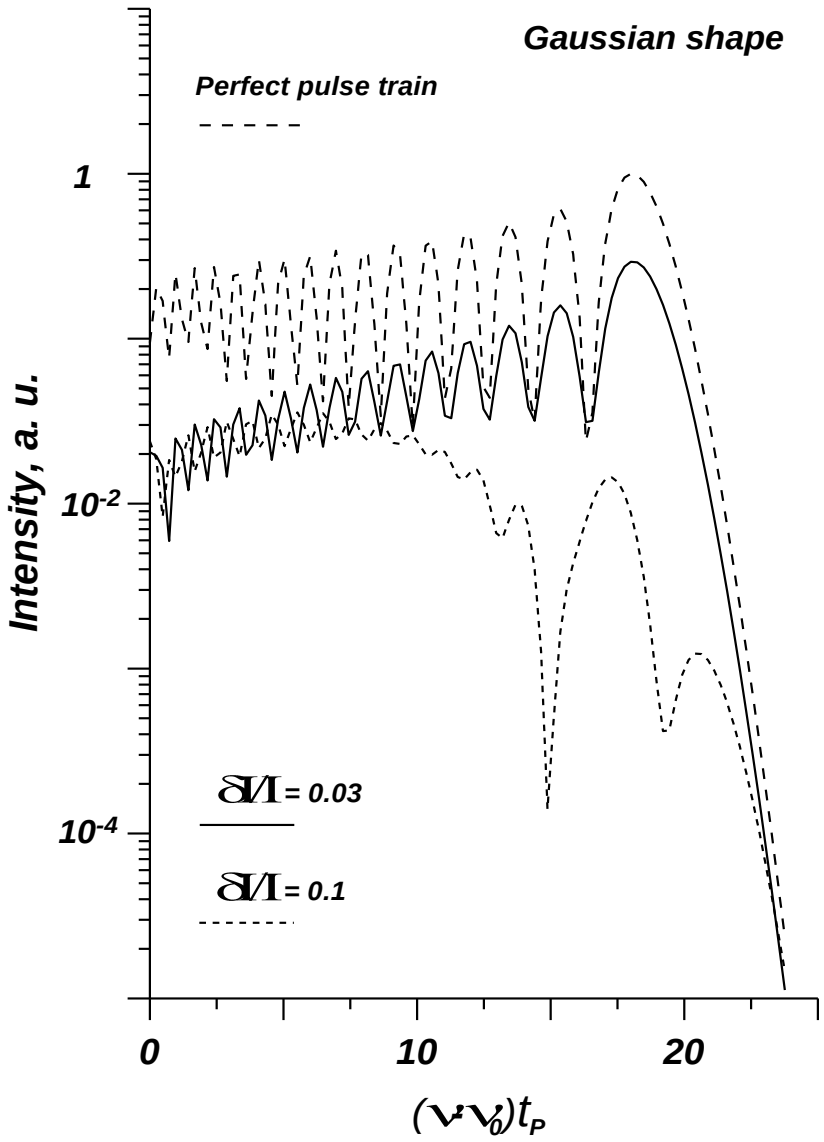

Figure 25. Spectral broadening of a Gaussian pulse train with amplitude instability. Pulse duration 30 fs., $\xi = \frac{z_{eff}}{L_{NL}} = 10^2$. Envelopes are normalized by the maximal spectral amplitude of a perfect pulse train.

Apparent nonconservation of energy is due to the calculation method. Spectra show only peak amplitudes of the comb, while in fact decrease of the spectral amplitudes in unstable pulse trains is compensated by the noise growth. Estimated ratio of noise and total spectral power depending on the level of intensity fluctuations is shown on Figure 26.

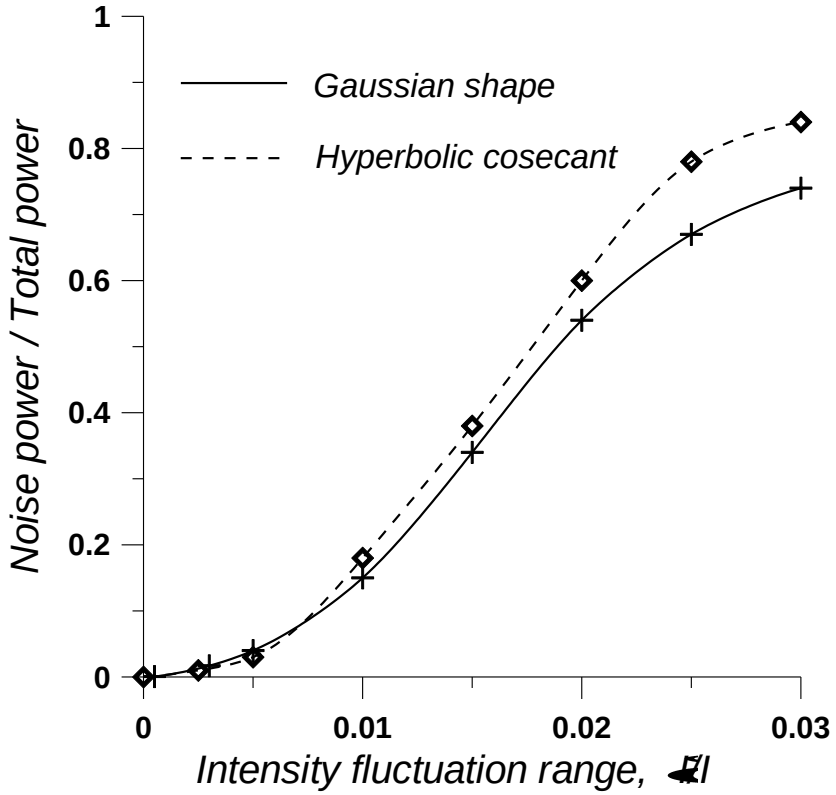

Fig. 26. Noise power and intensity fluctuations.

Since experimental measurements of the spectral envelope detect integral intensity over a relatively large intervals, embracing a number of components, they also include a noise part. Thus, numerical and experimental envelopes should be different, while comb amplitudes should be the same.

Intensity noise in HNLF: interplay between self-phase modulation and dispersion

Here we present numerical results obtained using the model described in the previous section. Typical numerical spectra are shown of Figure 27. As it can be seen, the significant difference between perfect and perturbed spectra, as it was in the case of SPM-only model, remains. Figure 28 shows spectra of two pulses within the same perturbed train.

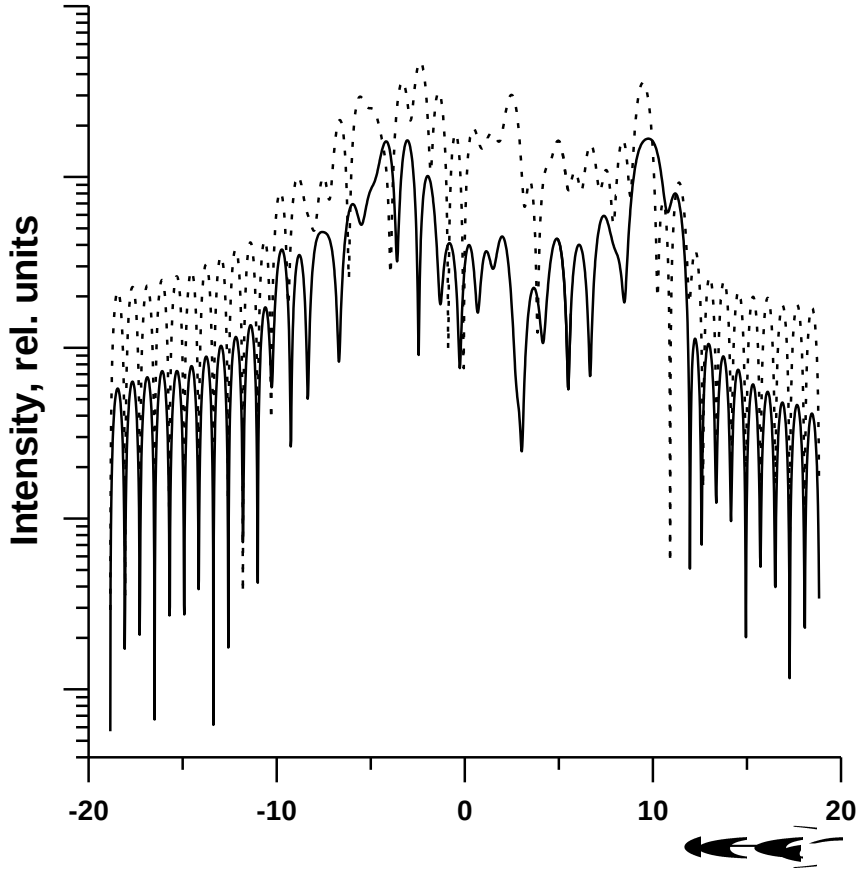

Figure 27. Unstable (solid) and perfect (dotted) pulse train spectra, calculated with an interplay between SPM and dispersion; $\beta_2 = -20\,ps^2/km$, $\beta_3 = \beta_2\tau$, $\tau = 30\,fs$, $\xi = z/L_{NL} = 10^2$, $N_p = 10^2$, $T_0 = 10^{-8}\,s$, amplitude fluctuations $\langle \delta I \rangle / I = 3 \cdot 10^{-2}$ with normal distribution.

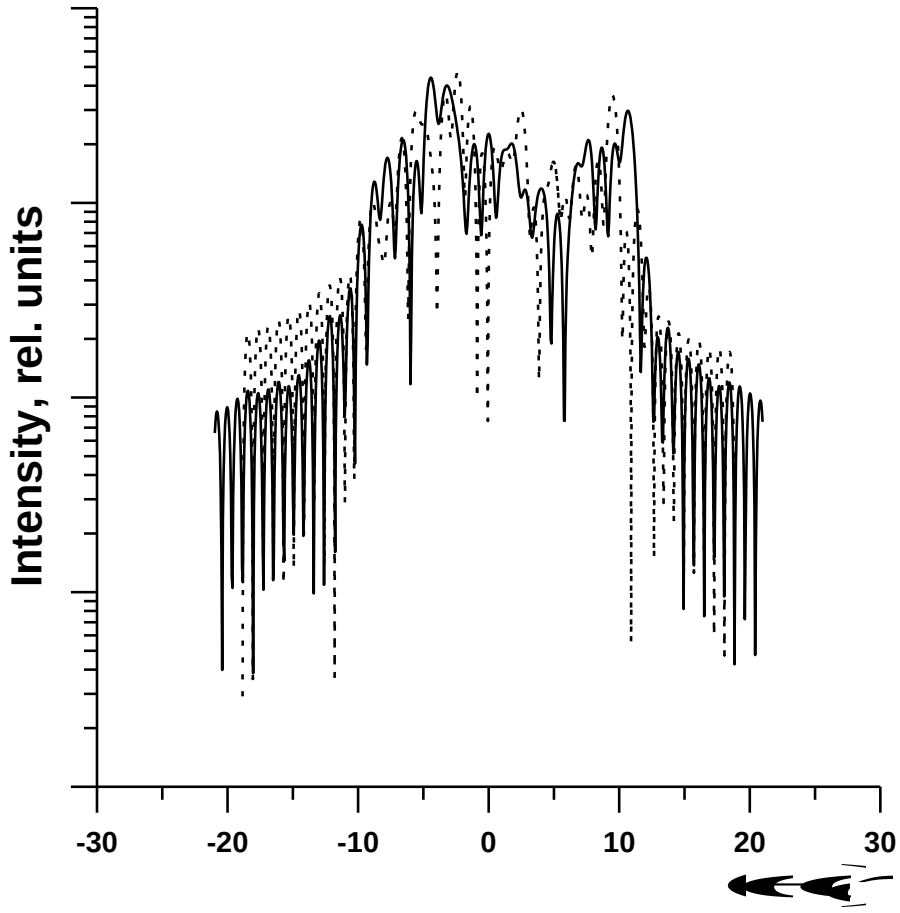

Figure 28. Spectra of two different pulses within a train, $\frac{|I_1 - I_2|}{\langle I \rangle} \approx 10^{-2}$.

It is also possible to estimate noise contribution by comparison of total spectrum area (i.e. area under spectral envelope) of perfect and perturbed trains. Fig. 28 shows dependence of noise power, which is a difference of perfect and perturbed train spectral areas, from the fluctuation amplitudes. It should be noted that integration over time confirms conservation of energy, but since noise widen comb components, it also reduces their amplitudes.

Figure 29 shows that dispersion plays an important role in spectral distortion. We could assume that dispersion should decrease amplitude noise influence, since it restricts spectral broadening and smoother multi-peak interference structure, however this occurs only for high fluctuations – greater than $3 \cdot 10^{-2}$, and only when dispersion is normal. When intensity variations are low, dispersion increases spectral noise. It can be seen that for all considered parameters, except the case of anomalous dispersion, noise power is more or less close, while anomalous dispersion gives a rise to the noise power when fluctuation amplitudes are small.

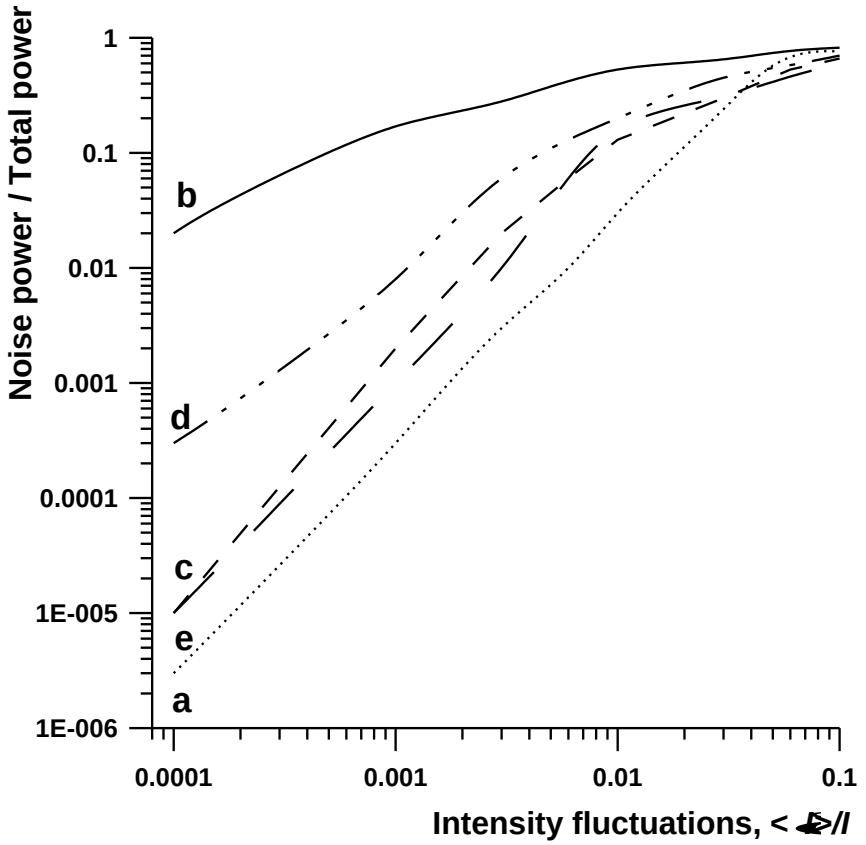

Figure 29. Noise part of total power, depending on the amplitude of intensity fluctuations. a – without dispersion (only SPM); b ($\beta_2 = -20 ps^2/km, \beta_3 = \beta_2\tau$) and d ($\beta_2 = -2 ps^2/km, \beta_3 = \beta_2\tau$) – anomalous dispersion; ($\beta_2 = 20 ps^2/km, \beta_3 = \beta_2\tau$) and e ($\beta_2 = 2 ps^2/km, \beta_3 = \beta_2\tau$) – normal dispersion; $\tau = 30 fs$, $\xi = z/L_{NL} = 10^2$, $N_p = 10^2$, $T_0 = 10^{-8} s$, amplitude fluctuations $\langle \delta I \rangle / I = 3 \cdot 10^{-2}$ with normal distribution.

Pulse train spectral broadening for a different pulse shapes

Figures 30a and 30b show broadened spectra of Gaussian and hyperbolic cosecant pulse trains with intensity fluctuations after propagation in fiber with strong self-phase modulation, calculated for 1000 pulses. Qualitative estimations show that for the typical experimental parameters of tapered fiber and Ti:S laser radiation 1-10% intensity stability and thus - nonlinear phase uncertainty leads to considerable spectral distortions.

It can be seen that even for a perfect pulse trains of different shapes spectral envelopes are very different. For a Gaussian shape we have a relatively small spectral values near the zero frequency (i.e. in the center of a spectrum) and high values on the border, while hyperbolic cosecant shows the opposite case, when maximal amplitudes are close to the center of spectrum (zero frequency detuning).

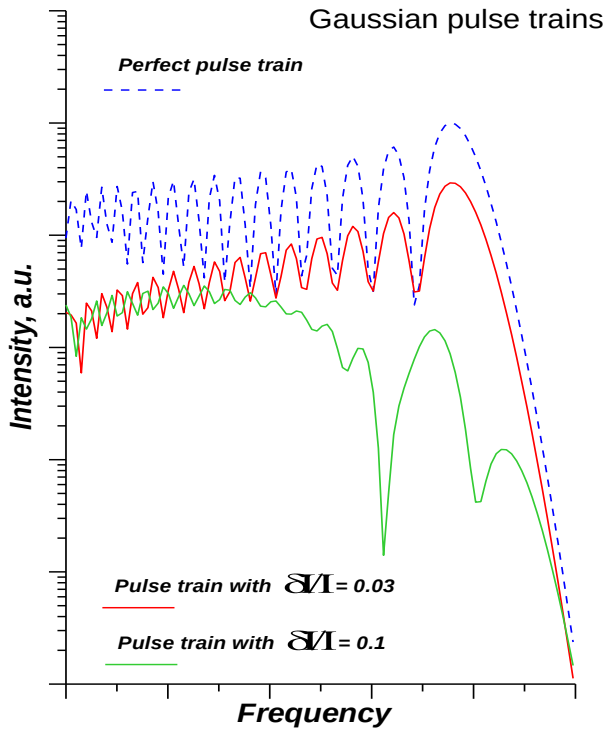

Figure 30a

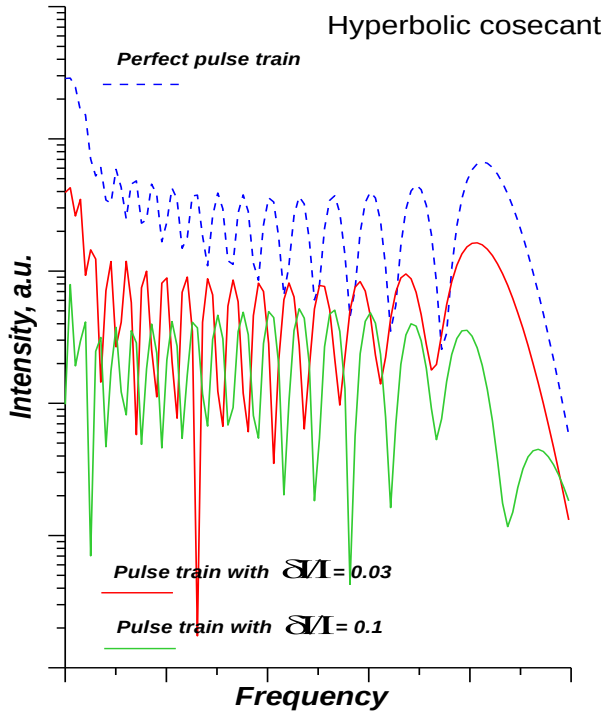

Figure 30b

Thus, the natural question is what happens if the pulse train is consisted of pulses with different shapes. Calculation of such a model is presented on the Figure 31.

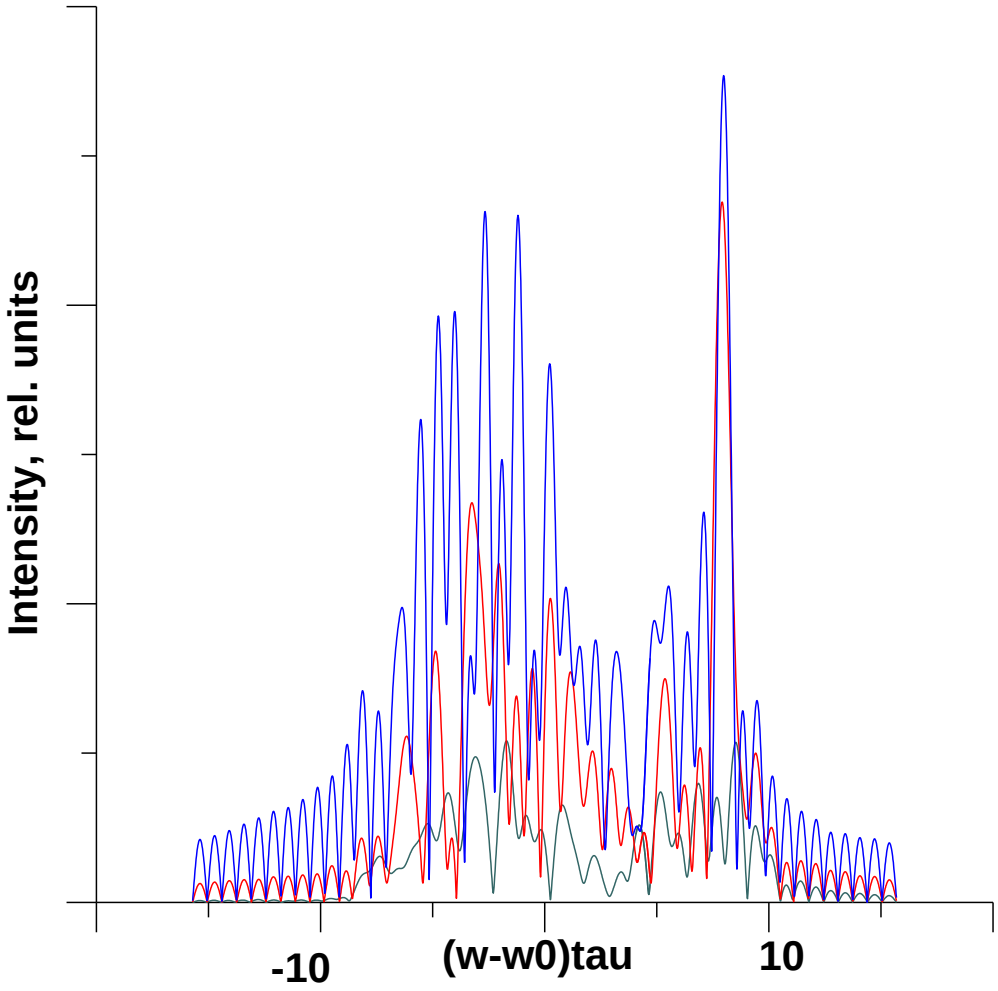

Figure 31. Broadened spectrum of a pulse train consisted of pulses with various shapes. Blue line – 100% Gaussian pulses; red line – 80% Gaussian and 20% hyperbolic cosecant; 50% of Gaussian and 50% of hyperbolic presented by a green line.

It was also found out that visible decrease of spectral components (envelope) in mixed pulse trains is compensated by the noise growth.

Results/Conclusions

The work on stabilization of the parameters of the femtosecond Cr:Forsterite laser has been accomplished. As a result a mechanically stable femtosecond forsterite laser with average output power of ~500 mW, pulse duration of ~40 fs and pulse repetition rate of 100 MHz has been developed. Work on increasing the Cr:Forsterite laser repetition rate from 100 MHz up to 200 – 300 MHz has been carried out.

Results on the development of a directly-diode-pumped Yb femtosecond laser have been reported. Various configurations of the compact laser cavity have been developed and analyzed. Laboratory stand for investigation of Yb lasers has been built. Investigations of ability to achieve of femtosecond operating regime in Yb:KYW based laser with 300-500 MHz repetition rate and using pump source UM3000/M10/CB TEC (Unique-mode) was carried out. For mode-locked regime stabilization semiconductor saturable mirror (BATOP Company) with modulation depth 2% was utilized. To compensate major part of gain medium dispersion GTI mirrors (Layertec) with negative dispersion were used. Non stationary generation regime was obtained.

Possible inaccuracy in DDF HNLF parameters determination and measurements indicates that in the frames of numerical modeling we can speak only about analysis of combined influence of nonlinear and dispersion factors on the base of NLSE solutions and about the most general tendencies of broadened spectrum formation. Nevertheless, in many cases numerical analysis makes it possible to describe experimental results. The most common conclusion is the ability to control spectral shape and to profile its envelope by varying fiber and input radiation parameters. Thus, numerical modeling is very useful for searching the optimal conditions of spectral broadening.

It was found that variability of a pulse intensities and shapes within the train can lead to a decrease of spectral components, which is similar to the case of spectral distortions in the presence of intensity fluctuations. It was also shown that, when dispersion is anomalous, spectral distortions are noticeable at much smaller fluctuation amplitudes.

In accordance with Defense Federal Acquisition Regulation 252.227-7036, Declaration of Technical Data Conformity (Jan 1997), "The Contractor, Dr. Denisov, hereby declares that, to the best of his knowledge and belief, the technical data delivered herewith under Contract No. FA8655-03-D-0001, DO 0028 is complete, accurate, and complies with all requirements of the contract.
DATE: November 20, 2008

Name and Title of Authorized Official (Project Director): V.I. Denisov, PhD, Leader Researcher and Scientific Secretary of Int. Aff. at ILPh
(2) In accordance with the requirements in Federal Acquisition Regulation 52.227-11, Patent Rights-Retention by the Contractor (Short Form) (Jun 1997),
"I certify that there were no subject inventions to declare as defined in FAR 52.227-11, during the performance of this order."
DATE: November 20, 2008

Name and Title of Authorized Official (Project Director): V.I. Denisov, PhD, Leader Researcher and Scientific Secretary of Int. Aff. at ILPh
The referenced Federal Acquisition Regulations can be found at http://farsite.hill.af.mil or http://www.arnet.gov/far/